

1 **Title**

2 Estimating maximum sustainable yield of snow crab (*Chionoecetes opilio*) off Tohoku Japan via a
3 state-space assessment model with time-varying natural mortality

4

5 **Authors**

6 Yasutoki Shibata^{1,2)}, Jiro Nagao²⁾, Yoji Narimatsu²⁾, Eisuke Morikawa²⁾, Yuto Suzuki²⁾, Shun Tokioka²⁾,
7 Manabu Yamada³⁾, Shigeho Kakehi⁴⁾, and Hiroshi Okamura⁵⁾

8

9 **Affiliations**

10 1) Japan Fisheries Research and Education Agency, 2-12-4 Fukuura, Kanazawa, Yokohama,
11 Kanagawa 236-8648, Japan

12

13 2) Hachinohe Laboratory, Tohoku National Fisheries Research Institute, Japan Fisheries Research and
14 Education Agency, Shimo-mekurakubo 25-259, Same, Hachinohe, Aomori, 031-0841, Japan

15

16 3) Fukushima Prefectural Research Institute of Fisheries Resources, 1-1-14 Koyo, Soma, Fukushima
17 976-0005, Japan

18

19 4) Shiogama Laboratory, Tohoku National Fisheries Research Institute, Japan Fisheries Research and
20 Education Agency, 3-27-5 Shinhama-cho, Shiogama, Miyagi 985-0001, Japan

21

22 5) National Research Institute of Fisheries Science, Japan Fisheries Research and Education Agency,
23 2-12-4 Fukuura, Kanazawa, Yokohama, Kanagawa 236-8648, Japan

24

25 **Corresponding author**

26 Yasutoki Shibata

27 shibatayas@affrc.go.jp

28 tel: +81 45 788 7615

29 fax: +81 45 788 5001

30

31 **Abstract**

32 Yield from fisheries is a tangible benefit of ecosystem services and sustaining or restoring a fish stock
33 level to achieve a maximum sustainable yield (MSY). Snow crab (*Chionoecetes opilio*) off Tohoku
34 has been managed by a total allowable catch since 1996, although their abundance has not increased
35 even after 2011, when fishing pressure rapidly decreased because of the Great East Japan Earthquake.
36 This implies that their biological characteristics, such as recruits, natural mortality coefficient (M), and

37 terminal molting probabilities (p), might have changed. We developed “just another state-space stock
38 assessment model (JASAM)” to estimate the MSY of the snow crab off Tohoku, Japan, considering
39 interannual variations in M and p . The multi-model inference revealed that M increased from 0.2 in
40 1997 to 0.59 in 2018, although it was not different among the instars, sex, nor terminal molt of crabs.
41 The parameter p also increased by 1.34–2.46 times depending on the instar growth stages from 1997
42 to 2018. We estimated the MSYs in three scenarios, which drastically changed if M and p were set as
43 they were in the past or at the current values estimated from this study. This result indicated that the
44 MSY of snow crab would also be time-varying based on their time-varying biological characteristics.

45

46 **Keywords**

47 Probability of terminal molt, random walk, stock assessment, the Great East Japan Earthquake, time-
48 varying ecosystem services

49

50 **Introduction**

51 Ecosystem services are the benefits that nature can provide to households, communities, and
52 economies (Boyd and Banzhaf 2006), and fish production (yield) is a tangible benefit of ecosystem
53 services (Tomscha and Gergel 2016). Although the development of fishery and transportation
54 technologies has become a factor to increase yield, an increase in yield may lead to overfishing and

55 reduced yield. At the United Nations summit in 2015, the Sustainable Development Goals (SDGs) was
56 adopted in “The 2030 Agenda for Sustainable Development” as a common international objective
57 from 2016 to 2030 (UN General Assembly 2015a). The SDGs comprise 17 goals and 169 targets, and
58 maintaining or restoring fish stock levels to achieve a maximum sustainable yield (MSY) as
59 determined by their biological characteristics is one of main targets of the SDGs (UN General
60 Assembly 2015b).

61 In Japan, the Fisheries Law has been amended for the first time in 70 years since it was enacted in
62 1949. In the amended Fisheries Law, it is necessary to set a target for fish abundance that maintains
63 the MSY of a (spawning stock) biomass calculated under natural conditions in the present and
64 reasonably foreseeable future (Fisheries Agency;
65 <https://www.jfa.maff.go.jp/j/kikaku/kaikaku/attach/pdf/suisankaikaku-20.pdf> last
66 accessed 29 January 2020). Some fish stocks that are legally managed by regulated total allowable
67 catch (TAC) have begun to be managed under this amended Fisheries Law.

68 Snow crab (*Chionoecetes opilio*) off the Tohoku region (Figure 1) have been managed by a total
69 allowable catch (TAC) since 1996, and are one of the most valuable exploited species in Japan. In
70 snow crab, terminal molting stops body growth as it matures (Yoshida 1941; Conan and Comeau
71 1986). At present, it is assumed that snow crab off Tohoku molt once a year in and after instar VI,
72 and then molt finally from instar X; this is based on a case study in which specimens from the Sea of

73 Japan were reared (Kuwahara et al. 1995).

74 Although total landings in the Tohoku area were around 100 gross ton before the 2011, total
75 landings and fishing efforts (the number of tows that caught at least one snow crab by bottom trawl
76 vessels) rapidly decreased in 2012 (Figure 2) because of the Great East Japan Earthquake and tsunami
77 in March 2011, which destroyed much of the fisheries-related infrastructure, such as fishing vessels,
78 fishing ports, and marine product processing factories. Fishing efforts for snow crab after the
79 earthquake have been less than 2% of those before 2011 (Shibata et al. 2019). Regarding bottom trawl
80 fishing off Fukushima, only trial fishing has been carried out since 2011 (Shibata et al. 2017).

81 The stock status of snow crab has been assessed by scientists of the Japanese Fisheries Research and
82 Education Agency (FRA), based on their estimated abundance (fishable biomass, males: only for
83 carapace width (cw) ≥ 80 mm, females: only for matured) by a swept area method from the survey
84 results of a research vessel (R/V) every year. Regardless of the quite low fishing efforts, the observed
85 abundance has continued decreasing rather than increasing, contrary to expectations (Figure 2).
86 Because fishing pressures have been kept quite low since March 2011, other factors have caused this
87 continued decrease. In fact, the two-year projected abundances that were needed to calculate the
88 allowable biological catch (ABCs) had likely been overestimated since 2012 by a previously
89 developed model (Ueda et al. 2009), with the fishing mortality coefficient (F) set as almost zero
90 (Shibata et al. 2019). One possible reason for this overestimation is that the biological characteristics,

91 such as recruits, natural mortality coefficient (M), and terminal molting probability (p), could have
92 changed in recent years. Especially, M and p might have increased and maintained high values; the
93 previous model assumed that M and p did not vary with time.

94 Since we are interested in the time variation of the parameters, it is necessary to estimate these
95 parameters using an appropriate statistical model. In previous studies, these parameters were treated
96 as constant with time, or expressed with random effects (Yamasaki 1988; Szuwalski and Turnock
97 2016; Murphy et al. 2018). However, it is more natural to assume that the parameters change
98 continuously rather than randomly changing every year. Therefore, we assumed that the biological
99 characteristic parameters followed a random walk (RW). A state-space stock assessment model (SAM)
100 has been reported (Nielsen and Berg 2014), in which some parameters vary by an RW process.
101 Although an age-structured model, such as statistical catch at age (SCAA), usually assumes that a
102 selectivity pattern is constant over time (Butterworth and Rademeyer 2008), SAM can estimate a time-
103 varying selectivity following an RW with a multivariate normal distribution (Nielsen and Berg 2014).
104 SAM also enables the use of information criteria, such as Akaike's information criterion (AIC) (Akaike
105 1974), for model selection, as opposed to the penalized likelihood approach (Nielsen and Berg 2014).
106 Since the model developed in this study has some structures in common with SAM, it will be called
107 JASAM (just another SAM).

108 The purpose of this study is to develop a state-space model that considers variations and predicts the

109 future abundance based on the stock–recruitment relationship defined in this study, thereby estimating
110 the MSY of snow crab off the Tohoku region, Japan, taking into account interannual variations in
111 biological characteristic parameters, such as recruits, M , and p .

112

113 **Materials and Methods**

114 *Scientific bottom trawl surveys*

115 To estimate the abundance of snow crab, scientific surveys using a bottom trawl net by the R/V
116 Wakataka-maru have been carried out between 1997 and 2018 on the northern part of Honshu Island,
117 Japan (Tohoku region [Figure 1]). A total of 150 survey stations were set to tow at depths from 150 to
118 900 m from September to November, where the spatial distribution of snow crab was at depths ranging
119 from 150 to 700 m and the main distribution range of fishable crabs (males with $cw \geq 80$ mm and
120 mature females) is approximately 400–550 m (Kitagawa 2000). The total length and mouth width of
121 the trawl net were 44.1 m and 5.4 m, respectively. The mesh size of the net was 50 mm and a cover
122 net with an 8 mm mesh was set at the cod-end. All tows were carried out during the daytime at a mean
123 ship speed of 3.0 knots for 30 min. The tow area (i.e., survey effort) of each station was calculated by
124 recording the arrival and departure point on the bottom and horizontal open width of the net using the
125 Net Recorder system (Furuno Electric Co., Hyogo, Japan or Marport, Reykjavik, Iceland).

126 The caught crabs were divided into males and females, and the number of individuals was counted.

127 For males, the *cw* and right (if not available, left) cheliped height was measured to the nearest 0.01
128 mm using a digital caliper (CD67-A20PM, Mitsutoyo, Kanagawa, Japan) to identify their maturity
129 (Watson 1970; Fujita et al. 1988). For females, the *cw* was also measured and recorded, and the
130 abdominal pleon was observed to determine maturity; adult females are characterized by a broad
131 abdominal pleon after terminal molt (Yoshida 1941). Instars of snow crabs off Tohoku were
132 distinguished by their *cw* intervals (Table 1) (Ueda et al. 2007). In snow crab, the number of molts
133 after instar VI is once a year; this can be used as an age trait (Kuwahara et al. 1995). The minimal
134 instar of the snow crab obtained by this scientific bottom trawl was instar VIII, where their interval of
135 *cw* is 24–42 mm (Table 1).

136 We then calculated the density at the station and estimated the total number at instar (*na*) with their
137 coefficients of variation (CVs) for the whole Tohoku region by multiplying by the area based on a
138 swept area method (Shibata et al. 2019). CVs were corrected by Taylor's power law (Supporting
139 Information 1). The estimated catch efficiency (Hattori et al. 2014) of the trawl net and their variance–
140 covariance matrix were used to estimate an unbiased abundance (see below eq. [34]).

141

142 *Catch data*

143 Snow crab have only been caught off the coast of the Tohoku region by offshore bottom trawl
144 fisheries (> 17 gross ton); their annual catches of snow crab were therefore used as a total catch. The

145 catch statistics were distinguished for males (only for $c_w \geq 80\text{mm}$) and females (only for matured).
146 Crabs were sampled and their c_w measured to reflect a whole composition of c_w in the total catch by
147 the Fukushima Fisheries Experimental Station. Additionally, their right or left cheliped height (only
148 for male) and maturity (only for female) were measured. Then, catch at instar (ca) was calculated
149 based on the instar and maturity composition in the sample data. Because Fukushima Prefecture
150 occupied 78% of fish catches (on average) of the total catch during 1997–2018 (Figure 2), the
151 representativeness of the samples was guaranteed. Samples during 1997–1998 and 2003 were not
152 available because the sample sizes were small, therefore the instar and maturity composition in 1999
153 and an average composition of 2002 and 2004 were used, respectively. Sample data during 2008–2010
154 were also not available because a hard disk containing those data was lost to the massive tsunami in
155 March 2011. Therefore, a composition of 2007 data was used to obtain ca values for those years.
156 Because there were few catches and measurements were not carried out from 2011 to 2017,
157 compositions of this period were substituted by those of the scientific bottom trawl survey. In 2018,
158 ca was available because measurements were carried out by scientists working for the FRA and
159 Fukushima Prefectural Research Institute of Fisheries Resources.

160

161 *Statistical modeling*

162 We developed a state-space stock assessment model coupled with an RW process, such as fishing

163 mortality coefficient (F) used in the SAM (Nielsen and Berg 2014). We hereafter refer to it as “just
164 another state-space stock assessment model” (JASAM). In JASAM, M and p can be stably estimated
165 because the number at instar and maturity have been obtained based on the scientific bottom trawl
166 survey. JASAM has two model structures, state and observation models, for the modeling of latent
167 population dynamics and the catch (observation) process. Unlike in SAM, not only F , but also M and
168 p , can have RW schemes in this model (see below).

169

170 Modeling of natural mortality coefficient

171 *Definition of M at group*

172 There are six instar categories, where a ($a = 8, \dots, 13$) shows the instar. Although we are interested
173 in an instar-specific natural mortality rate M_a , the adjacent instars may take the same M because
174 individuals of adjacent instars have similar body sizes, habitats, and are exposed to similar
175 environments. In this study, instar group g ($g = 0, \dots, 5$) was used to select M at group (M_g) and
176 instars were categorized for all groups (Supporting Information 2). The group consisted of
177 successive instar groups. For example, if instar VIII and X are in the same group, instar IX is also in
178 the same group. Since there are five “partitions” between one and six as integers and the same group
179 cannot be formed across the partitions, $2^5 = 32$ combinations were made for M_g .

180

181 *Time-varying M*

182 As we explained in the introduction, it was suspected that M and/or p have maintained a high value
183 in recent years. Considering the possibility that M varies with time, variations in M were assumed to
184 be one of the following three patterns: a constant, an RW of first-order difference, or that of second-
185 order difference. In the constant style, $M_{g,t+1} = M_{g,t} = M_g$ where t shows year ($t = 1997, \dots, 2018$). In
186 the first-order RW style,

187

$$188 \ln(M_{g,t+1}) \sim \text{Normal}(\ln(M_{g,t}), \sigma_{M,g}^2), \quad (1)$$

189

190 where σ_M is the standard deviation of the normal distribution used for RW. In the second-order RW
191 style, this is shown as

192

$$193 \ln(M_{g,t+1}) \sim \text{Normal}(2\ln(M_{g,t}) - \ln(M_{g,t-1}), \sigma_{M,g}^2). \quad (2)$$

194

195 These three patterns of $M_{g,t}$ were selected by model selection (see below).

196

197 *M after the terminal molting*

198 We categorize the number of years elapsed after the terminal molting, j ($j = 0, 1, 2$), into immature
199 ($j = 0$), terminally molted within one year ($j = 1$), and terminally molted after more than one year (j
200 $= 2$) (Shibata et al. 2019). The crabs mature functionally at the same time that they undergo the
201 terminal molt and cease to grow. Then, since the shells of snow crab have started to harden
202 gradually, M can be lower than that of an immature crab (Yamasaki 1988; Yamasaki et al. 1992). In
203 the stock assessment of snow crab, it has been assumed that M decreases for individuals one year
204 after terminal molting ($j = 2$). Therefore, M of an individual one year after the terminal molt was
205 multiplied by a multiplier φ ($0 < \varphi < 1$) to express the change in M after the terminal molt:

206

$$207 \quad M'_{g,t} = \begin{cases} M_{g,t}, & \text{if } j < 2, \\ M_{g,t}\varphi, & j = 2, \end{cases} \quad (3)$$

$$208 \quad \varphi = \frac{1}{(1 + \exp(-T_\varphi))}, \quad (4)$$

209 where $M_{g,t}$ is the natural mortality rate corresponding to the number of years elapsed after the
210 terminal molting and T_φ is a parameter that should be estimated.

211

212 Modeling of fishing mortality coefficient

213 Because the spatial distribution of snow crab off Tohoku is basically divided between mature and
214 immature individuals by sex rather than instar (Kitagawa 2000), F at instar has not been estimated in

215 the stock assessment in Japan (Shibata et al. 2019). We also use fishing mortality F , specified by

216 maturity status and sex. The time-varying F is shown below:

217

$$218 \quad \ln(F_{k,t+1}) = \begin{cases} \ln(F_{k,t}) + EQ_k + \varepsilon_{k,t}, & \text{if } t = 2010, \\ \ln(F_{k,t}) + \varepsilon_{k,t}, & \text{otherwise,} \end{cases} \quad (5)$$

219

220 where $k = 1$ (immature male), $k = 2$ (mature male), and $k = 3$ (mature female). When t is 2010, the

221 rapid decrease in fishing pressure due to the earthquake cannot be expressed by RW; therefore, it is

222 estimated as a fixed effect EQ . Here,

223

$$224 \quad \varepsilon_{k,t} \sim \text{MVN}(0, \Sigma_F), \quad (6)$$

225

226 where ε follows a multivariate normal (MVN) distribution, and its variance–covariance matrix Σ_F is

227 shown as

228

$$229 \quad \Sigma_F = [\rho_k \sigma_k^F \sigma_k^F] \\ 230 \quad = \begin{pmatrix} (\sigma_{k=1}^F)^2 & & \\ \rho_1 \sigma_{k=1}^F \sigma_{k=2}^F & (\sigma_{k=2}^F)^2 & \\ \rho_3 \sigma_{k=3}^F \sigma_{k=1}^F & \rho_2 \sigma_{k=2}^F \sigma_{k=3}^F & (\sigma_{k=3}^F)^2 \end{pmatrix}. \quad (7)$$

231

232 Here, upper triangular components were omitted and ρ and σ' were changed after 2011 as below:

233

$$234 \quad \rho_k = \begin{cases} \frac{1}{1+\exp(-T_{\rho_k})}, & \text{if } t < 2011, \\ \frac{1}{1+\exp(-(T_{\rho_k}+T_\rho))}, & \text{otherwise.} \end{cases} \quad (8)$$

235

$$236 \quad \ln(\sigma_k^F) = \begin{cases} \ln(\sigma_k^F), & \text{if } t < 2011, \\ \ln(\sigma_k^F) + T_{\sigma_k^F}, & \text{otherwise.} \end{cases} \quad (9)$$

237

238 Here, T_ρ is tested for whether it is zero in a model selection (see below), although T_σ is not, because

239 the total catch has apparently decreased and therefore T_σ must be changed after 2011. Model

240 selection was also carried out for ρ_k in five cases: one case that all ρ_k are one (i.e., T_{ρ_k} is not

241 estimated), three cases that two of the three ρ_k take the same value, and one case that all ρ_k are

242 different.

243

244 Modeling of terminal molt probability

245 The terminal molt probability (p) was modeled as a function of the instar; p may vary with time. We

246 modeled p using an RW process, as below:

247

$$248 \quad p_{a,t} = 1 / \left(1 + \exp \left(-(\beta_{0,t} + \beta_1 \times a) \right) \right), \quad (10)$$

$$249 \quad \beta_{0,t+1} \sim \text{Normal}(\beta_{0,t}, \sigma_{\beta_0}). \quad (11)$$

250

251 We carried out model selection to determine whether $\beta_{0,t} = \beta_0$ (i.e., not time-varying but constant) or

252 $\beta_{0,t}$.

253

254 State model of male

255 The structure of snow crab population dynamics is quite complex because they have six-plus groups

256 after instar X and the male fishable size ($cw \geq 80$ mm) divided instar XI (cw interval is 74–86 mm)

257 into two categories (Table 1). We hereafter describe the model formulae of each transition step by

258 step. Here, the initial number (i.e., in $t = 1997$) of snow crab at instar and sex were parameters to be

259 estimated.

260

261 *From instar VIII to IX ($a = 8$)*

262 The number at instar from instar VIII to IX can be shown as below:

263

264 $\ln(N_{a+1,j=0,t+1}) = \ln(N_{a,j=0,t}) - M'_{g,t}$ (12)

265

266

267 *From instar IX to X ($a = 9$, immature)*

268 From instar IX to X, some individuals mature (undergo terminal molting). The population dynamics

269 model can be expressed as

270

$$271 \quad \ln(N_{a+1,j=0,t+1}) = \ln(N_{a,j=0,t}) - M'_{g,t} + \ln(1 - p_{a,t}), \quad (13)$$

272

273 where $1 - p_{a,t}$ is the probability that an individual is not terminally molted.

274

275 *From instar IX to X (a = 9, mature)*

276 Terminal molting at instar X results in maturing with a *cw* of less than 80 mm, and the individual

277 ends its life without recruiting to a stock. The dynamics from immature to mature are shown as

278

$$279 \quad \ln(N_{a+1,j=1,t+1}) = \ln(N_{a,j=0,t}) - M'_{g,t} + \ln(p_{a,t}). \quad (14)$$

280

281 A plus group of instar X is shown as below:

282

$$283 \quad \ln(N_{a+1,j=2,t+1}) = \ln\left(\sum_{j=1}^2 N_{a+1,j,t} \exp(-M'_{g,t})\right). \quad (15)$$

284

285

286 *From instar X to XI (a = 10, immature)*

287 Since male snow crabs with a *cw* larger than 80 mm are fishable, the number of crabs at instar XI
288 (74–86 mm) multiplied by r ($0 < r < 1$) are fishable. In other words, the number of crabs at instar XI
289 were separated into ranges (74–80 mm as not fishable and 80–86 mm as fishable). Although we had
290 assumed that r was 0.5 in a previous study (Shibata et al. 2019), we estimated r in this report.

291 Individuals of instar XI with a *cw* of 74–80 mm without terminal molting can be modeled as

292

$$293 \ln(N_{a+1,j=0,t+1,74-80}) = \ln(N_{a,j=0,t}) - M'_{g,t} + \ln(1 - p_{a,t}) + \ln(1 - r). \quad (16)$$

294

295 The individuals of instar XI with a *cw* of 80–86 mm without terminal molting is then modeled as

296

$$297 \ln(N_{a+1,j=0,t+1,80-86}) = \ln(N_{a,j=0,t}) - M'_{g,t} + \ln(1 - p_{a,t}) + \ln(r), \quad (17)$$

298

299 where $r = 1/(1 + \exp(-Tr))$ and $N_{a+1,j=0,t+1} = N_{a+1,j=0,t+1,74-80} + N_{a+1,j=0,t+1,80-86}$.

300

301 *From instar X to XI (a = 10, mature)*

302 Individuals of instar XI with a *cw* of 74–80 mm with terminal molting are modeled as

$$303 \ln(N_{a+1,j=1,t+1,74-80}) = \ln(N_{a,j=0,t}) - M'_{g,t} + \ln(p_{a,t}) + \ln(1 - r), \quad (18)$$

304 $\ln(N_{a+1,j=2,t+1,74-80}) = \ln(\sum_{j=1}^2 N_{a+1,j,t,74-80} \exp(-M'_{g,t})).$ (19)

305

306 Individuals of instar XI with a *cw* of 80–86 mm with terminal molting are modeled as

307 $\ln(N_{a+1,j=1,t+1,80-86}) = \ln(N_{a,j=0,t}) - M'_{g,t} + \ln(p_{a,t}) + \ln(r),$ (20)

308 $\ln(N_{a+1,j=2,t+1,80-86}) = \ln(\sum_{j=1}^2 N_{a+1,j,t,80-86} \exp(-M'_{g,t} - F_{k=2,t})),$ (21)

309

310 where individuals that had experienced terminal molting were caught with a fishing mortality

311 coefficient of F .

312

313

314 *From instar XI to XII (a = 11, immature)*

315 Of the 74–80 mm and 80–86 mm individuals at instar XI, only the latter is subject to catch and is

316 expressed as follows:

317

318 $\ln(N_{a+1,j=0,t+1}) = \ln((N_{a,j=0,t,74-80} \exp(-M'_{g,t}) +$

319 $N_{a,j=0,t,80-86} \exp(-M'_{g,t} - F_{k=1,t}))(1 - p_{a,t}).$ (22)

320

321

322 *From instar XI to XII (a = 11, mature)*

323 Because the 80–86 mm individuals are terminally molted and included into a plus group of instars as

$$324 \ln(N_{a+1,j=1,t+1}) = \ln((N_{a,j=0,t,74-80} \exp(-M'_{g,t}) + N_{a,j=0,t,80-86} \exp(-M'_{g,t} - F_{k=1,t}))p_{a,t}),$$

$$325 \quad (23)$$

$$326 \ln(N_{a+1,j=2,t+1}) = \ln(\sum_{j=1}^2 N_{a+1,j,t} \exp(-M'_{g,t} - F_{k=2,t})). \quad (24)$$

327

328

329 *From instar XII to XIII (a = 12, immature)*

330 The number at instar from instar XII to XIII not terminally molted can be shown as below:

$$331 \ln(N_{a+1,j=0,t+1}) = \ln(N_{a,j=0,t}) - M'_{g,t} - F_{k=1,t} + \ln(1 - p_{a,t}). \quad (25)$$

332

333

334 *From instar XII to XIII (a = 12, mature)*

335 The number at instar from instar XII to XIII terminally molted can be shown as below:

$$336 \ln(N_{a+1,j=1,t+1}) = \ln(N_{a,j=0,t} \exp(-M'_{g,t} - F_{k=1,t})p_{a,t}), \quad (26)$$

$$337 \ln(N_{a+1,j=2,t+1}) = \ln(\sum_{j=1}^2 N_{a+1,j,t} \exp(-M'_{g,t} - F_{k=2,t})). \quad (27)$$

338

339

340 *From instar XIII to XIV (a = 13)*

341 Because all individuals at this instar stage mature at probability one, the equation is shown as below:

342

343 $\ln(N_{a+1,t+1}) = \ln(N_{a,j=0,t} \exp(-M'_{g,t} - F_{k=1,t})) +$

344 $\sum_{j=1}^2 N_{a+1,j,t} \exp(-M'_{g,t} - F_{k=2,t}).$ (28)

345

346

347 State model of female

348 *From instar VIII to IX and IX to X (a = 8 and 9, immature)*

349 Because females do not mature at instar X, the population transition is described as

350

351 $\ln(N_{a+1,j=0,t+1}) = \ln(N_{a,j,t}) - M'_{g,t} \exp(T_{Mg}),$ (29)

352

353 where T_{Mg} is the female-specific term, although T_{Mg} is tested for whether the term is zero or not.

354

355

356 *From instar X to XI (a = 10, immature)*

357 In females, because only instar XI is fishable, the transition is shown as below:

358

$$359 \quad \ln(N_{a+l,t+l}) = \ln(N_{a,j=0,t} \exp(-M'_{g,t} \exp(T_{M_g}))) +$$

$$360 \quad \sum_{j=1}^2 N_{a+l,j,t} \exp(-M'_{g,t} \exp(T_{M_g}) - F_{k=2,t}). \quad (30)$$

361

362

363 *Estimation of the number of individuals at instar VIII*

364 Because our survey can observe snow crabs older than instar VIII, we treated the number of

365 individuals at instar VIII as recruits. Here, we assumed an RW process as below:

366

$$367 \quad \ln(N_{a=8,j=0,t+1}) \sim \text{Normal}(\ln(N_{a=8,j=0,t}), \sigma_{rec}^2), \quad (31)$$

368

369 where the numbers of males and females were assumed to be the same (i.e., the sex ratio of recruits

370 was assumed as 0.5).

371

372

373 Observation model

374 *Scientific bottom trawl survey*

375 The estimated number of individuals in the trawl survey n is obtained by multiplying the catch

376 efficiency q by the true number of individuals N . Elapsed years after the terminal molting are not
377 known by the trawl survey; only the identification before or after the terminal molting ($u = 0$ where j
378 $= 0$, $u = 1$ where $j = 1$ and 2) can be determined. An observation model for the trawl survey is shown
379 as below:

380

$$381 \quad \ln(n_{a,u,t}) \sim \text{Normal}(\ln(q_{a,t} N_{a,u,t}^{\theta_0 + \theta_1 + \theta_2 a}), \log(1 + \omega_{a,u,t}^2) + \log(1 + CV_{a,u,t}^2)), \quad (32)$$

$$382 \quad \ln(\omega_{a,u,t}) \sim \text{Normal}(\mu_\omega, \sigma_\omega^2), \quad (33)$$

383

384 where θ_0 – θ_2 are parameters of hyperstability (or hyperdepletion) that show a nonlinear relationship
385 between abundance and its index (Hilborn and Walters 1992; Chen et al. 2008), and θ_1 is only
386 estimated for females. To make the model flexible, we treated ω^2 as a random effect term. We
387 calculated the likelihood as both $n_{a,u,t,74-80}$ and $n_{a,u,t,80-86}$ for males, although the suffix was omitted in
388 eq. (32). The CV of the number of individuals estimated by the swept area method is used in eq. (32).

389 The catch efficiency q is shown as below:

390

$$391 \quad q_{a,t} = \gamma_0 / (1 + \exp(-(\gamma_2 + \gamma_3 c w_{a,t}))), \quad (34)$$

$$392 \quad \gamma_0 = 1 / (1 + \exp(-\gamma_1)), \quad (35)$$

393

394 where $cW_{a,t}$ was the average cW of each instar obtained from the annual trawl survey. The catch
395 efficiency $q_{a,t}$ was treated as a random effect term and the average γ_1 – γ_3 and their variance–covariance
396 matrix was plugged in from the previous study (Hattori et al., 2014).

397

$$398 \quad \gamma_h \sim \text{MVN}(\hat{\gamma}_h, \Sigma_\gamma), \quad (36)$$

399

$$400 \quad \Sigma_\gamma$$
$$401 \quad = \begin{pmatrix} 0.214 & & & \\ -0.003 & 8.758 \times 10^{-5} & & \\ 0.002 & -0.001 & 0.074 & \\ & & & \end{pmatrix}. \quad (37)$$

402

403 Here, upper triangular components were omitted and $\hat{\gamma}_1 = 0.683$, $\hat{\gamma}_2 = -4.276$, and $\hat{\gamma}_3 = 0.0792$.

404

405

406 *Catch at instar*

407 c_a is the observed number of catch at instar and C_a is the estimated number of catch at instar; these

408 were shown as below:

409

$$410 \quad \ln(c_{a,u,t}) \sim \text{Normal}(\ln(C_{a,u,t}), \tau_{a,u}^2), \quad (38)$$

$$411 \quad C_{a,u=0,t} = N_{a,u=0,j=1,t} \exp(-M'_{g,t}/6) (1 - F_{k=1,t}) w_{a,u=0,t}, \quad (39)$$

$$412 \quad C_{a,u=1,t} = \sum_{j=1}^2 N_{a,u=1,j,t} \exp(-M'_{g,t}/6) (I - F_{k,t}) w_{a,u=1,t}, \quad (40)$$

413

414 where the catch of male snow crab was applied using both eq. (39) and (40) ($k = 2$), although that of
415 females was applied using eq. (40) ($k = 3$) alone, because only mature females were caught.

416

417 Model selection

418 *State and observation models*

419 There are eight factors to be selected in the model: 1) The variables/types of difference in M_g to be
420 selected were 32 combinations for M_g (Supporting Information 2), 2) three types of difference for $M_{g,t}$,
421 3, 4) either φ and $T_{Mg} = 1$ or not, 5) either $T_\rho = 0$ or not, 6) five combinations for $T_{\rho k}$, 7) either β_0 was
422 time-varying or not, and 8) either the parameters of hyperstability were included in model or not (Table
423 2). Consequently, the number of tested models is 15,360 ($=32 \times 3 \times 2 \times 2 \times 2 \times 5 \times 2 \times 2$). The number
424 of parameters for $M_{g,t}$ were all about whether a constant (M_g), a first-order difference (σ_{M^2g}), or a
425 second-order difference (σ_{M^2g}) model was selected, because the number of parameters equaled the
426 number of groups. The first-order difference may be selected more easily than the other two types
427 because it is considered to be the most flexible for fitting. We therefore performed model selection for
428 each of three types for $M_{g,t}$ and selected the best one by both AIC (Akaike 1974) and Bayes'
429 information criterion (BIC) (Schwarz 1978). Six models will ultimately be chosen as candidates for

430 the best model through this procedure.

431 The estimated abundance A_{T-i} ($A = \sum_a N_a W_a$, $T = 2018$, $i = 1, \dots, 5$) of both males and females was
432 calculated using all the data from 1997 to 2018. The estimated abundance using the data period from
433 1997 to $T-i$ ($i = 1, \dots, 5$) was denoted as A_{T-i, R_i} ($R_i = R_1, \dots, R_5$), where R_i is a suffix indicating how
434 many years of data are excluded. As an index representing retrospective bias, Mohn's rho (ρ_{past}) (Mohn
435 1999) was calculated by the following equation:

436

$$437 \quad \rho_{past} = \frac{1}{5} \sum_{i=1}^5 \left(\frac{A_{T-i, R_i} - A_{T-i}}{A_{T-i}} \right) \times 100. \quad (41)$$

438

439 In addition, a retrospective forecasting (Brooks and Legault 2015) approach was used to estimate an
440 error in future projections for two years ahead because the ABC of snow crab had been calculated
441 based on data from two years ago (Shibata et al. 2019). First, the abundance was estimated using the
442 data from 1997 to $T-j$, excluding the data for j years ($j = 3, \dots, 7$). Then \tilde{A}_{T-h, R_h} ($h = j - 2$) was
443 projected for the abundance two years ahead. For example, when $j = 3$ then $h = 1$, the abundance and
444 the parameter estimation were performed using the data up to 2015, and the abundance in 2017 was
445 predicted. This procedure was repeated to calculate ρ_{future} for ABC using the following formula:

446

$$447 \quad \rho_{future} = \frac{1}{5} \sum_{h=1}^5 \left(\frac{\tilde{A}_{T-h, R_h} - A_{T-h}}{A_{T-h}} \right) \times 100. \quad (42)$$

448

449 All parameter values were given their average over the past three years to calculate ρ_{future} . Biases in
450 the estimation and prediction of the abundance for the six best models were evaluated using ρ_{past} and
451 ρ_{future} and the best model was selected. As a sensitivity test, the CVs of the observed number of instars
452 were multiplied by 1.5 using the best model. We then calculated ρ_{past} , ρ_{future} , and time-varying $M_{g,t}$.

453

454

455 *Stock–recruitment relationship*

456 We fitted three types of stock–recruitment (SR) relationship between the estimated spawning stock
457 biomass (SSB) and recruitment (instar VIII) that were obtained from the best model from the above
458 model selection phase for future predictions. We used three types of SR relationships as hockey stick
459 (HS) (Clark et al. 1985), Beverton–Holt (Beverton and Holt 1957) (BH) and Ricker (RI) (Ricker 1954)
460 models for eq. (43), (44), and (45), respectively, as below:

461

$$462 \quad \hat{R}_{t+5} = \begin{cases} \alpha_0 SSB_t & \text{if } SSB_t < \alpha_1 \\ \alpha_0 \alpha_1 & \text{if } SSB_t \geq \alpha_1 \end{cases}, \quad (43)$$

$$463 \quad \hat{R}_{t+5} = \frac{\alpha_0 SSB_t}{1 + \alpha_1^{-1} SSB_t}, \quad (44)$$

$$464 \quad \hat{R}_{t+5} = \alpha_0 SSB_t \exp(-\alpha_1^{-1} SSB_t), \quad (45)$$

465

466 where t is year ($t = 1997, \dots, 2013$). In snow crab, although there is no information on the length of
467 each instar duration in the Tohoku region, it has been assumed that five years are needed to reach instar
468 VIII in the Sea of Japan (Ueda et al. 2007), and we assumed this to be true in these equations. SSB is
469 the spawning stock biomass after a fishing season and is calculated as below:

470

$$471 \quad SSB_t = \left(N_{a,u=1,t} \exp(-M_{g,t}) - c_{a,u=1,t} \exp\left(-\frac{5}{6}M_{g,t}\right) \right) w_{a,u=1,t}, \quad (46)$$

472

473 where N , c , and w are the estimated number, observed catch number, and mean weight of mature
474 female, respectively. α_0 and α_1 are parameters to be estimated by maximizing the log likelihood (LL)
475 function for each model, as below:

476

$$477 \quad \eta_t = \log(R_{t+5}) - \log(\hat{R}_{t+5}), \quad (47)$$

$$478 \quad \sigma_{SR} = \sqrt{\frac{1}{n} \sum_{t=2002}^{2018} \eta_t^2}, \quad (48)$$

$$479 \quad LL = \log\left(\prod_{t=1997}^{2013} \frac{1}{\sqrt{2\pi\sigma_{SR}^2}} \exp\left(-\frac{\eta_t^2}{2\sigma_{SR}^2}\right)\right). \quad (49)$$

480

481 Snow crab could have a warm and cold regime for their recruitment in the eastern Bering Sea
482 (Szuwalski and Punt 2013). Although it has not been reported surrounding Japan, we considered the
483 case that an autocorrelation existed in residuals (η) to express the regime of recruitment, as shown

484 below:

485

$$486 \quad \eta_t = \rho_{SR}\eta_{t-1} + \xi_t, \quad (50)$$

$$487 \quad \xi_t \sim \text{Normal}(0, (1 - \rho_{SR}^2)\sigma_{SR}^2), \quad (51)$$

$$488 \quad \sigma = \sqrt{\frac{1}{n} \left\{ \eta_{t=2002}^2 + \frac{1}{1 - \rho_{SR}^2} \sum_{t=2003}^{2018} (\eta_t - \rho_{SR}\eta_{t-1})^2 \right\}}. \quad (52)$$

489

490 Here, we did not estimate α_0 , α_1 , and ρ_{SR} simultaneously because it had been reported that estimates
491 would be unstable and bias could arise (Johnson et al. 2016). In summary, we carried out a model
492 selection using AICc (Hurvich and Tsai 1989) from the three SR relationships (i.e., α_0 and α_1 were
493 fixed). We then estimated ρ_{SR} and tested whether the autocorrelation in the residuals estimated for ρ_{SR}
494 was zero or not.

495

496

497 Estimation of maximum sustainable yield

498 Because M and p were time-varying, we defined their values used to estimate the MSY. We prepared
499 three scenarios in M and p as 1) the mean values during 2016–2018, 2) mean values during 1997–
500 1999, and 3) mean values among all years. In the future prediction, the best model of the SR
501 relationship was used. To estimate the MSY, we used the below equations for F :

502

$$503 \quad F_{k,latest} = \frac{1}{3} \sum_{t=2007}^{2009} F_{k,t}, \quad (53)$$

$$504 \quad F_{k,candi} = F_{k,latest} \times X, \quad (54)$$

$$505 \quad X = \frac{10}{1 + \exp(-x)}. \quad (55)$$

506

507 We changed x from -10 to 10 by 0.01 and $F_{k,candi}$ was used for the future prediction. The life expectancy
508 of snow crab in Newfoundland was reported to be 13 and 19 years old for females and males,
509 respectively (Comeau et al. 1998). Although it has not been studied in detail in Japan, snow crab life
510 expectancy was often assumed to be more than 10 years old (e.g., Shibata et al., 2019). We assumed
511 the life span of snow crab to be 15 years and simulated the future prediction as 20 times the life span
512 to obtain initial values of the population. We carried out the prediction for 400 years and the mean
513 catches between 301 and 400 years were recorded where the first 300 years were not used to delete
514 the effects of the initial values. We repeated this procedure $1,000$ times and calculated a median catch
515 each x (i.e., a mean catch between 301 and 400 years was obtained $1,000$ times each x and $2,001$
516 medians from the mean catches were obtained). Then, we selected the $F_{k,candi}$ that maximized the
517 medians of catch as F_{MSY} , and MSY and SSB_{MSY} were also obtained. The calculation was carried out
518 using freely available statistical analysis software R (R Core Team 2019) and the Template Model
519 Builder (TMB) (Kristensen et al. 2015).

520

521

522 **Results**

523 *The best models of state and observation models*

524 Models that had minimal AIC and BIC values are shown in Table 3. The result also showed the
525 combination of g , the variables included in a model, and values of retrospective analysis for each
526 model. The models with constant M_g through time were the same as each other regardless of the two
527 information criteria. The model showed that instars VIII and IX, and instars X, XI, and XII were the
528 same groups. The models with a first-order difference of M_g were the same whether the criterion was
529 AIC or BIC where instars VIII and IX, instars X and XI, and instars from XII to XIII were grouped,
530 respectively. The parameter T_{Mg} was selected in the model. The model had both the minimum AIC
531 (1,064.5) and BIC (1,254.2) among the three formulations of $M_{g,t}$. In the case of the model with a
532 second-order difference of M_g , both AIC and BIC had the smallest values when all of the age groups
533 were combined. In contrast, although the AIC minimal model contained three parameters (θ_0 – θ_2) that
534 considered hyperstability, the BIC minimal model did not. The parameter of terminal molting
535 probability β was selected as time-varying, and $T_{\rho k=1}$ was not different from $T_{\rho k=2}$ in all cases.

536 The values of ρ_{past} did not greatly change among models and were relatively small (Table 3). In
537 contrast, ρ_{future} showed poor performance except for in the BIC best model with a second-order

538 difference of $M_{g,t}$. Although the model with a first-order difference of $M_{g,t}$ had the smallest AIC and
539 BIC among the three formulations of $M_{g,t}$, we decided that the minimal BIC model with a second-
540 order difference of $M_{g,t}$ was the best model from the synthetic evaluation of model performance,
541 including retrospective bias and retrospective forecasting. All of the estimated parameter values of the
542 best model are shown in Table 4, and the results indicated that the estimated values were well fitted to
543 the observed values and the residuals showed normally distributed (Figure 3 and Supporting
544 Information 3)

545 Estimated time-varying $M_{g,t}$ and terminal molting probabilities from the best model were shown in
546 Figures 4 and 5, respectively. Although the time-varying $M_{g,t}$ was not so high in 1997 ($M_{g,t} = 0.20$),
547 values increased from around 2005 to 2012. The $M_{g,t}$ kept a high value of more than 0.59. This result
548 indicated that the abundance of snow crab could not increase if the total catch was kept at quite low
549 values after the earthquake because the natural mortality also kept a high value. Terminal molting
550 probability also kept increasing from around 2005 in all instars that had terminal molts (Figure 5).
551 Although the values were 0.09, 0.19, 0.38, and 0.61 in 1997 for each instar (IX, X XI and XII), these
552 values increased to 0.21, 0.41, 0.64, and 0.82 in 2017. This indicated that the terminal molting
553 probabilities increased 2.46-, 2.10-, 1.67-, and 1.34-fold, respectively from 1997 to 2018. This also
554 showed that the decreasing abundance was caused by both the high natural mortality and terminal molt
555 probability. The estimated abundance and SSB were shown in Figures 6 and 7, respectively. Both

556 results showed that estimated values kept decreasing after 2008 prior to the earthquake when estimated
557 fishing mortalities were kept quite low ($F = 0.04$ for immature male in 2016 was the maximum) after
558 2011 (Figure 8).

559

560 *Sensitivity analysis of CV*

561 The result showed that the $M_{g,t}$ did not change greatly even if CV was multiplied by 1.5 (Figure 9).
562 The ρ_{past} and ρ_{future} changed by this multiplication from 1.2% to -1.8% and from 3.1% to -6.1% ,
563 respectively (see also Table 3). This result showed that the estimates and predicted values were robust
564 against the CVs of the number of snow crabs observed by the scientific bottom trawl survey.

565

566 *Estimated MSY*

567 The HS model had the minimal AICc because the calculated AICc values were 29.9, 32.21, and 32.0
568 for the HS, BH, and RI SR models, respectively. The SR relationship estimated by the HS model and
569 estimated ρ_{SR} are shown in Figure 10a and 10b, respectively. Although the number of instar VIII crabs
570 as recruits decreased since 2015 (Figure 10a), the timing of the decrease was different from that of the
571 abundance (Figure 2). Because the estimated coefficient of autocorrelation was significantly different
572 from zero if the lag was one year (Figure 10b), we used the HS model with autocorrelation in the
573 residuals for future predictions to estimate MSYs based on the three scenarios. Here, the estimated

574 MSY and SSB_{MSY} are shown in Table 5. Although scenario 1 showed that the MSY and SSB_{MSY} were
575 quite high values that had not been experienced in the historical catch (Figure 2) and estimated SSB
576 (Figure 7), both MSY and SSB_{MSY} in scenario 2 were almost zero because the abundance was also
577 almost zero. In scenario 3, the MSY was low compared to the observed historical catch, although the
578 estimated SSB_{msy} was near to that of the median value from 1997 to 2018 (185.8 gross ton).

579

580

581 **Discussion**

582 In this study, we showed that the natural mortality coefficient M and the terminal molting probability
583 p of snow crab in the Tohoku region have increased since 1997. In their stock assessments, it was
584 assumed that $M = 0.35$ for individuals that have not experienced a terminal molt and for those that
585 have experienced a terminal molt within one year, and $M = 0.2$ for those that have undergone a terminal
586 molt two or more years ago (Shibata et al., 2019). In contrast, regardless of the time elapsed since the
587 terminal molt, it has been found in this study that M was around 0.59 as of 2018. This means that
588 previous stock assessments overestimated future survival. Indeed, it had been expected that abundance
589 would increase since 2011 because of the rapid decline in total catch (Shibata et al., 2019), although
590 the abundance has maintained a declining trend (Figure 6) despite F being nearly zero (Figure 8).
591 Since F has been nearly zero and the scientific bottom trawl survey covered the whole habitat of snow

592 crab off Tohoku, the result of this estimation is naturally that M and the p have increased.

593 One potential cause for the increase of M could be an increased bottom water temperature (BWT).

594 The BWT data were not used in this model since the periods of the surveys were different from those

595 of BWT and we were interested in time-varying parameters thorough the bottom trawl survey period.

596 In contrast, it was suggested that the mean BWT in the Tohoku region was on an upward trend (Figure

597 11) and a method to draw Figure 11 is shown in Supporting Information 3. An aquarium study

598 indicated that the energy consumed inside the crab exceeds the energy absorbed from outside at a

599 water temperature of 7 °C; therefore it would be energetically impossible for the crab to live

600 persistently in this water temperature range (Foyle et al. 1989). In other words, the increased BWT off

601 Tohoku could be one reason for the increase in M . Although the main fishing ground for snow crab

602 has been concentrated in the area from the Miyagi to Ibaraki prefectures (Nemoto 2007), the area of

603 unsuitable environment for survival in the major distribution area of snow crab could have expanded

604 (Figure 11). In contrast, since the trends of BWT and M do not completely match, it seems that factors

605 other than the BWT are affecting M .

606 Another possible reason for the increase in M is predation pressure. It has been known that predation

607 pressure by Atlantic cod (*Gadus morhua*) affects the abundance of snow crab (Chabot et al. 2008).

608 In the Tohoku region, the abundance of Pacific cod (*Gadus macrocephalus*) had increased rapidly

609 since fishing pressure was decreased by the earthquake (Narimatsu et al. 2017) and snow crab have

610 been observed in their stomach contents; therefore, this may have affected the abundance of snow crab
611 (Ito et al. 2014). In contrast, the estimated natural mortality coefficient M was the same for all age
612 groups in this study. M should differ between small and large snow crabs if the predation pressure by
613 Pacific cod affects the rise in M . In fact, it has been reported that snow crabs larger than 65.1 mm
614 rarely appear in the stomach of Atlantic cod (Chabot et al. 2008). The abundance of Pacific cod peaked
615 in 2015 and started to decrease (Narimatsu et al. 2019); however, that of instar VIII snow crab has not
616 turned to an increasing trend, but rather decreased (Figure 10a). This indicates that the predation
617 pressure of Pacific cods is not a main reason for the increase in M of all instars.

618 Not only the natural mortality M , but also the terminal molting probability p , had increased. It has
619 been reported that the terminal molting probability of snow crab off Miyagi and Fukushima prefectures
620 were higher than that off Ibaraki Prefecture; this might be due to the fact that large individuals were
621 selectively caught under high fishing pressure, resulting in genetically smaller maturity size (Takasaki
622 and Tomiyama 2017). In contrast, this study showed that p has been on an upward trend even after
623 2011, when F decreased rapidly because of the earthquake. This therefore suggested that the terminal
624 molting probability would not fluctuate only by fishing mortality. One hypothesis is that recent
625 increases in BWT may affect p . Although several studies have reported a positive correlation between
626 water temperature and size-at-terminal molt (Somerton 1981; Alunno-Bruscia and Sainte-Marie 1998;
627 Zheng et al. 2001; Orensanz et al. 2007; Burmeister and Sainte-Marie 2010; Dawe et al. 2012;

628 Yamamoto et al. 2015); however, the Tohoku region has higher water temperatures than any previous
629 studies (Figure 11). It will be necessary to examine the size-at-terminal molt in relatively high-water
630 temperatures through an aquarium experiment.

631 Our study revealed that the value of MSY apparently changed when the values of M and the terminal
632 molting probability changed in three scenarios (Table 5). This suggests that the MSY as an ecosystem
633 service varies greatly with time, and that fishing pressure needs to be reduced to almost zero when M
634 and p are high. It has been reported that snow crab could have a warm and cold regime for recruitment
635 in the eastern Bering Sea and show drastic stock fluctuation (Szuwalski and Punt 2012, 2013). This
636 study revealed, even in the Tohoku region, the possibility of dynamic stock fluctuations regardless of
637 changes in fishing pressure, because M and terminal molting probability varied with time. Although
638 recruits were decreased since 2015 (Figure 10a), this was not the main reason for decreased abundance
639 (Figure 2) because instar VIII as recruits needed at least three more years to be fishable (i.e., instar
640 XI). In other words, the decreased trend in abundance since 2012 was not caused by the decreased
641 recruits since 2015, but by M and p . Although the catch of snow crab has been limited because bottom
642 trawlers in Fukushima prefecture voluntarily decreased the effort of fishing, the effort should not
643 increase in the future if M and p maintain high values.

644 Because the study design allowed for the estimation of M and p , we could show that ecosystem
645 services can vary with time. Although changes in production due to global warming have been pointed

646 out around the world (Free et al. 2019), it could affect biological parameters, such as M and p . There
647 could be many species other than snow crab whose biological parameters vary with the environment
648 in the seas around Japan, but there are few examples where the biological parameters have been
649 actually estimated. Japan is currently moving to a new stock management targeting MSY, but it is
650 commonly assumed that the value of M has mainly been based on empirically derived equations and
651 does not change over time (Tanaka 1960). For species that are likely to be highly affected by the
652 environment, scientific survey designs to estimate abundance should be prepared to allow the
653 estimation of the parameters and capture of the temporal changes.

654 One of the features of JASAM is that it estimates parameters for population dynamics using the
655 annual abundance observed independently of fisheries. It is conceivable that the parameters will have
656 other specifications, such as an RW with a multivariate normal distribution, as in the case of F , and a
657 step function. It is also possible to change the state model for snow crab to another age-structured
658 model so that it can be applied to species other than snow crab. However, if the estimated abundance
659 does not reflect the entire distribution area of the target species, M can be confounded with migration
660 rates to adjacent sea areas. In this case, it may be necessary to assume the rates of migration to the off-
661 site area separately, or to design a survey (e.g., estimation of abundance in the adjacent sea areas) that
662 can estimate the rates of migration.

663

664 **Acknowledgment**

665 We thank the crew of the Wakataka-maru, Tanshu-maru, and Hokko-maru for their assistance in
666 obtaining samples. We also thank the staff of Hachinohe Laboratory, Tohoku National Fisheries
667 Research Institute, and Fukushima Prefectural Research Institute of Fisheries Resources for help in
668 preparing the samples. Dr Nishijima gave useful comments for methods to use the TMB. Mr Takahashi,
669 Mr Miharu, Mr Matsumoto, Mr Sato, and Mr Kaneko gave useful comments from the viewpoint of
670 the bottom trawl fishers of Fukushima. This study was funded by the Fisheries Agency of the Ministry
671 of Agriculture, Forestry, and Fisheries of Japan.

672

673

674 **References**

675 Akaike H (1974) A new look at the statistical model identification. In: Selected Papers of

676 Hirotsugu Akaike. Springer, pp 215–222

677 Alunno-Bruscia M, Sainte-Marie B (1998) Abdomen allometry, ovary development, and

678 growth of female snow crab, *Chionoecetes opilio* (Brachyura, Majidae), in the

679 northwestern Gulf of St. Lawrence. *Can J Fish Aquat Sci* 55:459–477

680 Beverton RJH, Holt SJ (1957) On the dynamics of exploited fish populations. Her Majesty's

681 Stationary Office, London

- 682 Boyd J, Banzhaf S (2006) What Are Ecosystem Services? The Need for Standardized
683 Environmental Accounting Units. *Ecol Econ* 63:616–626.
684 <https://doi.org/10.1016/j.ecolecon.2007.01.002>
- 685 Brooks EN, Legault CM (2015) Retrospective forecasting—evaluating performance of stock
686 projections for New England groundfish stocks. *Can J Fish Aquat Sci* 73:935–950
- 687 Burmeister A, Sainte-Marie B (2010) Pattern and causes of a temperature-dependent
688 gradient of size at terminal moult in snow crab (*Chionoecetes opilio*) along West
689 Greenland. *Polar Biol* 33:775–788
- 690 Butterworth DS, Rademeyer RA (2008) Statistical catch-at-age analysis vs. ADAPT-VPA:
691 the case of Gulf of Maine cod. *ICES J Mar Sci* 65:1717–1732
- 692 Chabot D, Sainte-Marie B, Briand K, Hanson JM (2008) Atlantic cod and snow crab
693 predator-prey size relationship in the Gulf of St. Lawrence, Canada. *Mar Ecol Ser -*
694 *MAR ECOL-PROGR SER* 363:227–240. <https://doi.org/10.3354/meps07384>
- 695 Chen Y, Jiao Y, Sun CL, Chen X (2008) Calibrating virtual population analysis for fisheries
696 stock assessment. *Aquat Living Resour* 21:89–97. <https://doi.org/10.1051/alr:2008030>
- 697 Clark CW, Charles AT, Beddington JR, Mangel M (1985) Optimal capacity decisions in a
698 developing fishery. *Mar Resour Econ* 2:25–53
- 699 Comeau M, Conan GY, Maynou F, et al (1998) Growth, spatial distribution, and abundance

- 700 of benthic stages of the snow crab (*Chionoecetes opilio*) in Bonne Bay, Newfoundland,
701 Canada. Can J Fish Aquat Sci 55:262–279
- 702 Conan GY, Comeau M (1986) Functional maturity and terminal molt of male snow crab,
703 *Chionoecetes opilio*. Can J Fish Aquat Sci 43:1710–1719
- 704 Dawe EG, Mullett DR, Moriyasu M, Wade E (2012) Effects of temperature on size-at-
705 terminal molt and molting frequency in snow crab *Chionoecetes opilio* from two
706 Canadian Atlantic ecosystems. Mar Ecol Prog Ser 469:279–296
- 707 Foyle TP, O’dor RK, ELNER RW (1989) Energetically defining the thermal limits of the
708 snow crab. J Exp Biol 145:371–393
- 709 Free CM, Thorson JT, Pinsky ML, et al (2019) Impacts of historical warming on marine
710 fisheries production. Science (80-) 363:979 LP – 983.
711 <https://doi.org/10.1126/science.aau1758>
- 712 Fujita H, Takeshita K, Matuura S (1988) Relative growth of chela and size at maturity in
713 Tanner crabs, *Chionoecetes oppilio* and *C.bairdi*. Res Crustac 17:7–13.
714 https://doi.org/10.18353/rcustacea.17.0_7
- 715 Hattori T, Ito M, Shibata Y, et al (2014) Net efficiency of a bottom trawl survey for snow
716 crab *Chionoecetes opilio* off the Pacific coast of northern Honshu, Japan. Nippon
717 Suisan Gakkaishi 80:178–184

- 718 Hilborn R, Walters CJ (1992) Quantitative fisheries stock assessment: choice, dynamics
719 and uncertainty. Chapman Hall, New York 570
- 720 Hurvich CM, Tsai C-L (1989) Regression and time series model selection in small samples.
721 *Biometrika* 76:297–307
- 722 Ito M, Hattori T, Narimatsu Y, Shibata Y (2014) Predation of snow crab *Chionoecetes opilio*
723 by Pacific cod *Gadus macrocephalus* off northeastern Honshu, Japan. *Tohoku sokouo*
724 *kenkyu* 34:123-132 (In Japanese)
- 725 Johnson KF, Councill E, Thorson JT, et al (2016) Can autocorrelated recruitment be
726 estimated using integrated assessment models and how does it affect population
727 forecasts? *Fish Res* 183:222–232
- 728 Kitagawa D (2000) Distribution and some biological characters of the snow crab
729 *Chionoecetes opilio* in the Pacific region of northeastern Honshu. *Bull Tohoku Natl*
730 *Fish Res Inst* 63:109-118 (in Japanese with English abstract)
- 731 Kristensen K, Nielsen A, Berg CW, et al (2015) TMB: automatic differentiation and Laplace
732 approximation. *J Stat Softw* 70:1–21
- 733 Kuwahara A, Shinoda M, Yamasaki A, Endo S (1995) Managements of the snow crab
734 resource in the western Japan sea. *Japan Fish Resour Conserv Assoc* 44:1–89
- 735 Mohn R (1999) The retrospective problem in sequential population analysis: An

- 736 investigation using cod fishery and simulated data. *ICES J Mar Sci* 56:473–488
- 737 Murphy JT, Rugolo LJ, Turnock BJ (2018) Estimation of annual, time-varying natural
- 738 mortality and survival for Eastern Bering Sea snow crab (*Chionoecetes opilio*) with
- 739 state-space population models. *Fish Res* 205:122–131
- 740 Narimatsu Y, Shibata Y, Hattori T, et al (2017) Effects of a marine-protected area occurred
- 741 incidentally after the Great East Japan Earthquake on the Pacific cod (*Gadus*
- 742 *macrocephalus*) population off northeastern Honshu, Japan. *Fish Oceanogr* 26:
<https://doi.org/10.1111/fog.12201>
- 743
- 744 Narimatsu Y, Shibata Y, Suzuki Y, et al (2019) Stock assessment and evaluation for the
- 745 Pacific cod stock of north Pacific off Honshu, Japan (fiscal year 2018). *Fish Agency*
- 746 *Fish Res Educ Agency Japan* 1083–1114
- 747 Nemoto Y (2007) Stock condition of snow crab *Chionoecetes opilio* from catch informations.
- 748 *Tohoku sokouo kenkyu* 27:54-60 (In Japanese)
- 749 Nielsen A, Berg CW (2014) Estimation of time-varying selectivity in stock assessments
- 750 using state-space models. *Fish Res* 158:96–101
- 751 Orensanz JM, Ernst B, Armstrong DA (2007) Variation of female size and stage at maturity
- 752 in snow crab (*Chionoecetes opilio*)(Brachyura: Majidae) from the eastern Bering Sea. *J*
- 753 *Crustac Biol* 27:576–591

- 754 R Core Team (2019) A language and environment for statistical computing
- 755 Ricker WE (1954) Stock and recruitment. *J Fish Board Canada* 11:559–623
- 756 Schwarz G (1978) Estimating the dimension of a model. *Ann Stat* 6:461–464
- 757 Shibata Y, Narimatsu Y, Suzuki Y, et al (2019) Stock assessment and evaluation for the
- 758 snow crab of northern Pacific stock (fiscal year 2018). In *Marine fisheries stock*
- 759 *assessment and evaluation for Japanese waters (fiscal year 2018/2019)*. Fish Agency
- 760 Fish Res Educ Agency Japan 493–556
- 761 Shibata Y, Sakuma T, Wada T, et al (2017) Effect of decreased fishing effort off Fukushima
- 762 on abundance of Japanese flounder (*Paralichthys olivaceus*) using an age-structured
- 763 population model incorporating seasonal coastal-offshore migrations. *Fish Oceanogr*
- 764 26: <https://doi.org/10.1111/fog.12179>
- 765 Somerton DA (1981) Regional variation in the size of maturity of two species of tanner crab
- 766 (*Chionoecetes bairdi* and *C. opilio*) in the eastern Bering Sea, and its use in defining
- 767 management subareas. *Can J Fish Aquat Sci* 38:163–174
- 768 Szuwalski C, Punt AE (2013) Regime shifts and recruitment dynamics of snow crab,
- 769 *Chionoecetes opilio*, in the eastern Bering Sea. *Fish Oceanogr* 22:345–354
- 770 Szuwalski C, Turnock J (2016) A stock assessment for eastern Bering Sea snow crab. *Stock*
- 771 *Assess Fish Eval Rep King Tann Crab Fish Bering Sea Aleutian Islands Reg* 167–251

- 772 Szuwalski CS, Punt AE (2012) Fisheries management for regime-based ecosystems: a
773 management strategy evaluation for the snow crab fishery in the eastern Bering Sea.
774 ICES J Mar Sci 70:955–967. <https://doi.org/10.1093/icesjms/fss182>
- 775 Takasaki K, Tomiyama T (2017) Geographic variation in the size-related terminal-molt
776 proportion and carapace width of the male snow crab *Chionoecetes opilio* off the
777 Pacific coast of southern Tohoku, Japan. Nippon Suisan Gakkaishi 83:156–162
- 778 Tanaka S (1960) Studies on the dynamics and the management of fish populations. Bull
779 Tokai Reg Fish Res Lab 28:1–200
- 780 Tomscha SA, Gergel SE (2016) Ecosystem service trade-offs and synergies misunderstood
781 without landscape history. Ecol Soc 21:1. <https://doi.org/10.5751/ES-08345-210143>
- 782 Ueda Y, Ito M, Hattori T, et al (2009) Estimation of terminal molting probability of snow
783 crab *Chionoecetes opilio* using instar- and state-structured model in the waters off the
784 Pacific coast of northern Japan. Fish Sci 75:47–54. [https://doi.org/10.1007/s12562-008-](https://doi.org/10.1007/s12562-008-0016-6)
785 0016-6
- 786 Ueda Y, Ito M, Hattori T, et al (2007) Growth of the snow crab *Chionoecetes opilio*
787 estimated by carapace width frequency analysis in the water off the Pacific coast of
788 northern Honshu, Japan. Nippon Suisan Gakkaishi 73:487–494
- 789 UN General Assembly (2015a) Transforming Our World: The 2030 Agenda for Sustainable

- 790 Development. A/RES/70/1
- 791 UN General Assembly (2015b) 69th Session. Agenda Item 13(a) [Last accessed on 2020 Jan
- 792 15]. https://www.un.org/ga/search/view_doc.asp?symbol=A/RES/70/1&Lang=E
- 793 Watson J (1970) Maturity, mating, and egg laying in the spider crab, *Chionoecetes opilio*. J
- 794 Fish Board Canada 27:1607–1616
- 795 Yamamoto T, Yamada T, Kinoshita T, et al (2015) Effects of temperature on growth of
- 796 juvenile snow crabs, *Chionoecetes opilio*, in the laboratory. J Crustac Biol 35:140–148
- 797 Yamasaki A (1988) Ecological Studies on Zuwai crab, *Chionoecetes opilio*, in the Sea off
- 798 Kyoto Prefecture-IV. Bull Kyoto Inst Ocean Fish Sci 35–42
- 799 Yamasaki A, Sinoda M, Kuwahara A (1992) Estimation of Survival Rate after Terminal
- 800 Molting of Male Snow Crab *Chionoecetes opilio*. Nippon Suisan Gakkaishi 58:181–186
- 801 Yoshida H (1941) On the reproduction of useful crabs in North Korea. Suisan Kenkyushi
- 802 36:116–123
- 803 Zheng J, Kruse GH, Ackley DR (2001) Spatial distribution and recruitment patterns of
- 804 snow crabs in the eastern Bering Sea. Spat Process Manag Mar Popul Ed by GH Krus
- 805 N Bez, A Booth, MW Dorn, S Hills, RN Lipcius, D Pelletier, C Roy, SJ Smith D
- 806 Witherell, Univ Alaska Sea Grant, Rep AK-SG-01-02, Fairbanks, AK 233–255
- 807

808 **Figure captions**

809

810 **Fig. 1**

811 Stations surveyed by the R/V Wakataka-maru since 1997 (black circles, 150 stations). The survey area
812 covered off Aomori, Iwate, Miyagi, Fukushima, and Ibaraki prefectures from 150 to 900 m depth.
813 Contours drawn by 100 m depth.

814

815 **Fig. 2**

816 Total catch (metric ton, bar graph), estimated abundance (metric ton) by a swept area method from
817 survey data of the R/V Wakataka-maru (black circles) and effort of bottom trawl vessels (number of
818 hauls, white triangles). Total catch was distinguished between that of Fukushima (gray) and other
819 prefectures (dark gray). Effort value in 2018 was under calculation.

820

821 **Fig. 3**

822 Relationship between observed and estimated values and histograms of residuals for the number of
823 snow crabs (a, b) and catch (c, d) of the best model.

824

825 **Fig. 4**

826 Estimated $M_{g,t}$ of the best model with a 95% confidential interval (break lines).

827

828 **Fig. 5**

829 Estimated $p_{a,t}$ of the best model with their 95% confidential intervals (break lines). The symbols

830 indicate those of instars IX (white circles), X (black circles), XI (white triangles), and XII (black

831 triangles).

832

833 **Fig. 6**

834 Estimated abundance of the best model with 95% confidential interval (break lines). The two

835 horizontal dashed lines show the minimum and maximum estimates before 2011.

836

837 **Fig. 7**

838 Estimated SSB after a fishing season of the best model with a 95% confidential interval (break lines).

839 The horizontal dashed line shows the minimum estimates before 2011.

840

841 **Fig. 8**

842 Estimated fishing mortalities of the best model by immature male (black squares), mature male (black

843 triangles), and mature female (white circles).

844

845 **Fig. 9**

846 Estimated $M_{g,t}$ (a) and calculated ρ_{past} (b) and ρ_{future} (c) after CV in eq. (32) was multiplied by 1.5. The

847 black and white circles in Fig. 9(a) show values before and after the multiplication, respectively.

848

849 **Fig. 10**

850 Estimation of the best SR relationship (a) and autocorrelation of their residuals (b) with 95%

851 confidential intervals (break lines).

852

853 **Fig. 11**

854 Estimated mean bottom water temperatures (BWT, °C) from January to December (i.e., 12 months) at

855 depths 300–400 m (a) and 400–500 m (b). Mean from November to December (i.e., two months) was

856 also calculated for each depth range (c and d) because the period was the warmest off Ibaraki prefecture

857 (the southern limit of snow crab distribution in the Tohoku region).

858

859

860

861 **Table captions**

862

863 **Table 1**

864 Relationships among carapace width, instar, terminal molting, and sex that decide if the crab is fishable

865 or not.

866

867 **Table 2**

868 Combination of all variables/types of difference for model selection.

869

870 **Table 3**

871 Results of the model selection and retrospective analysis. The column M showed three types of $M_{g,t}$

872 (constant, first-order, or second-order difference). M_g was same if the numbers expressed in columns

873 from VIII to XIII were the same. If the cell showed “In”, that indicated that the variable was selected

874 in the model by information criteria, and “-” showed that it was not selected. β was selected as p was

875 time-varying (indicated as “ t ”) in all cases.

876

877 **Table 4**

878 Estimated parameter values and their standard errors by the best second-order difference model.

879

880 **Table 5**

881 Estimated MSY and SSB_{MSY} for each scenario with their M values.

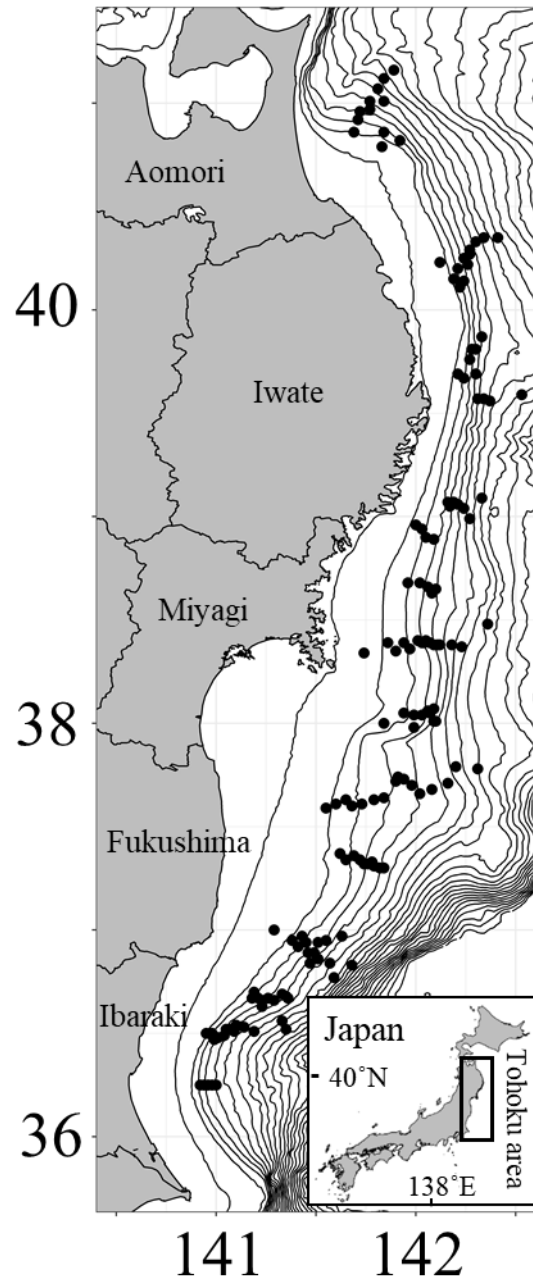
882

883

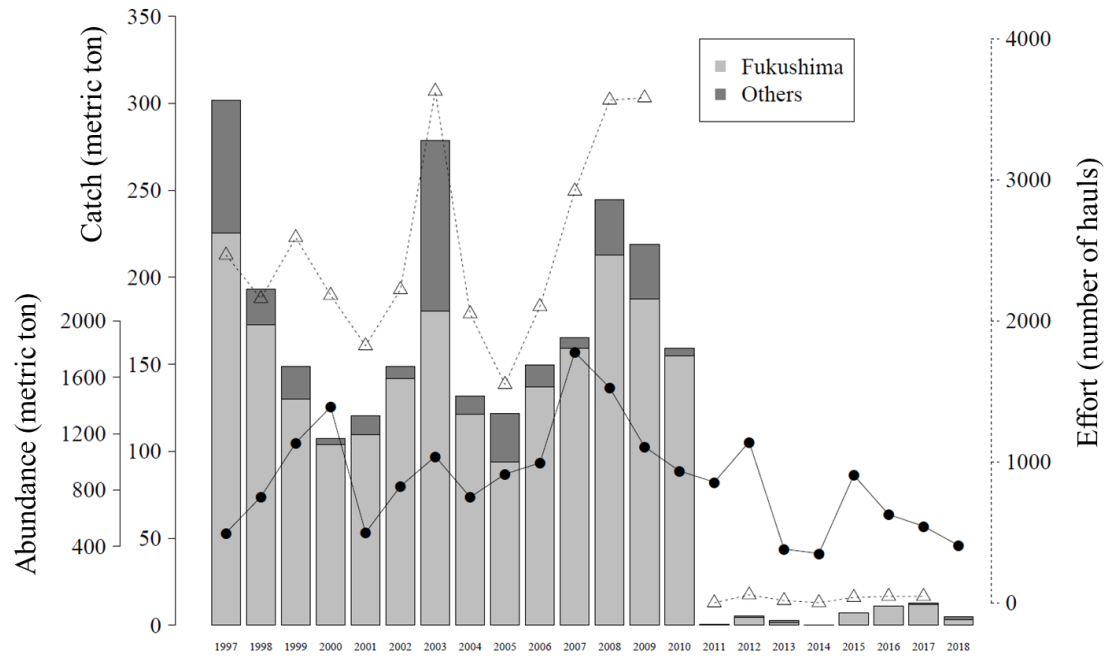
884

885

886



887 Fig. 1



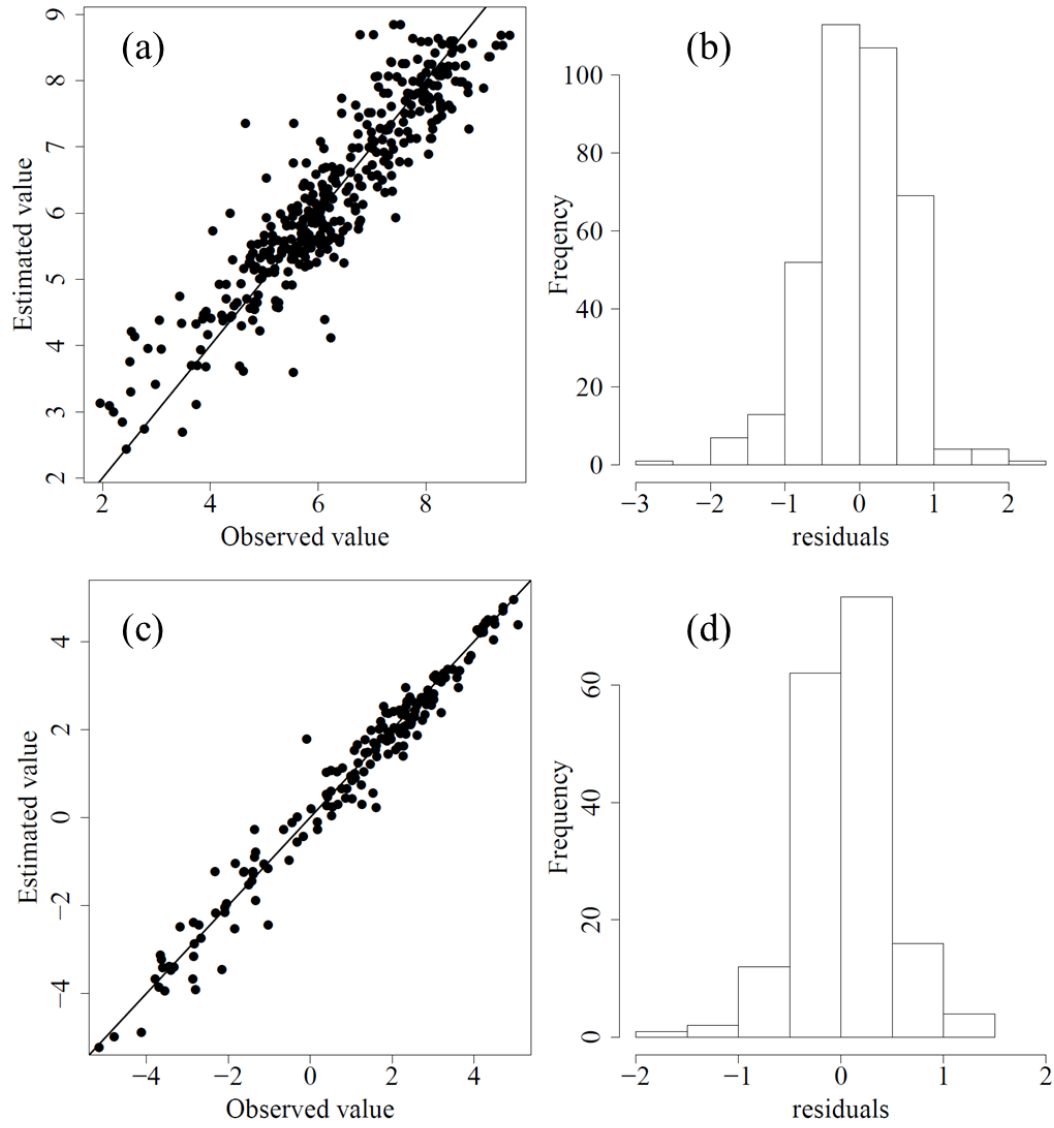
888

889

890

Fig. 2

891



892

893 Fig. 3

894

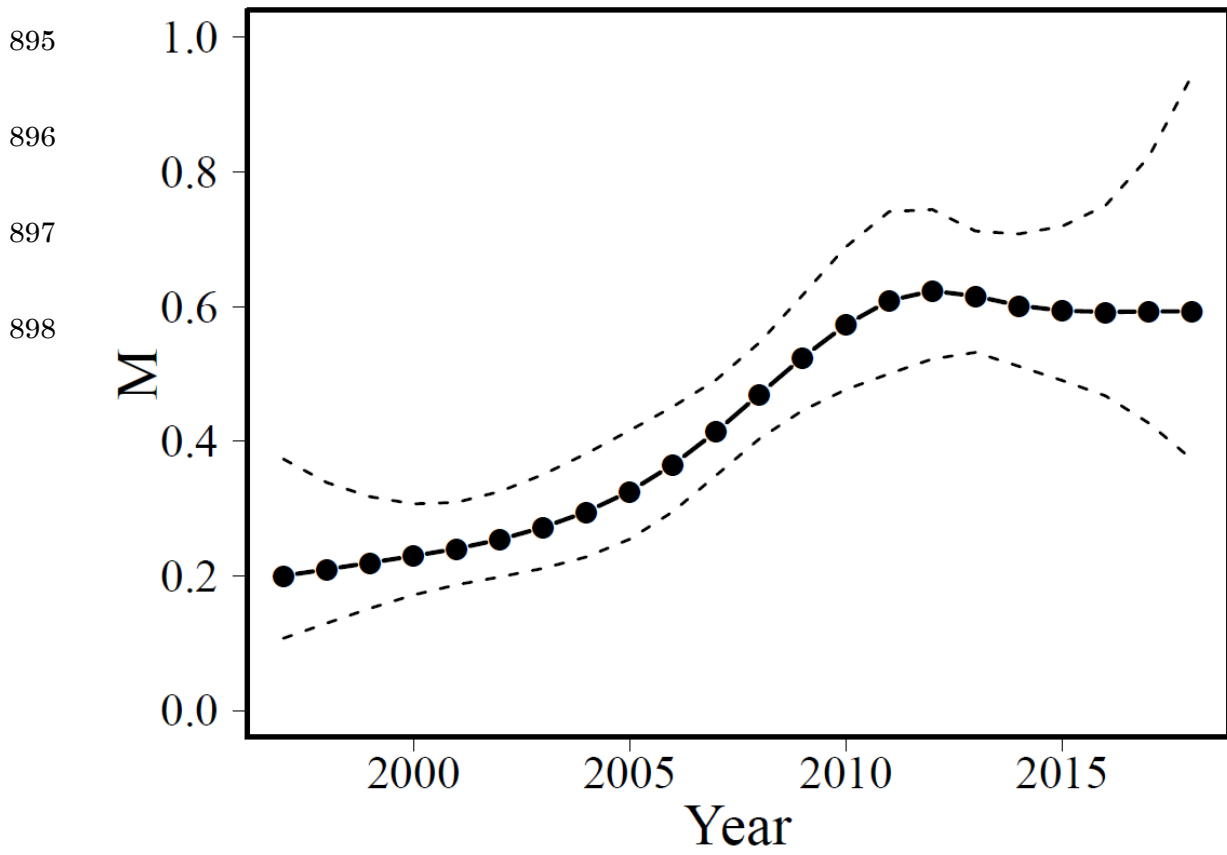


Fig. 4

899

900

901

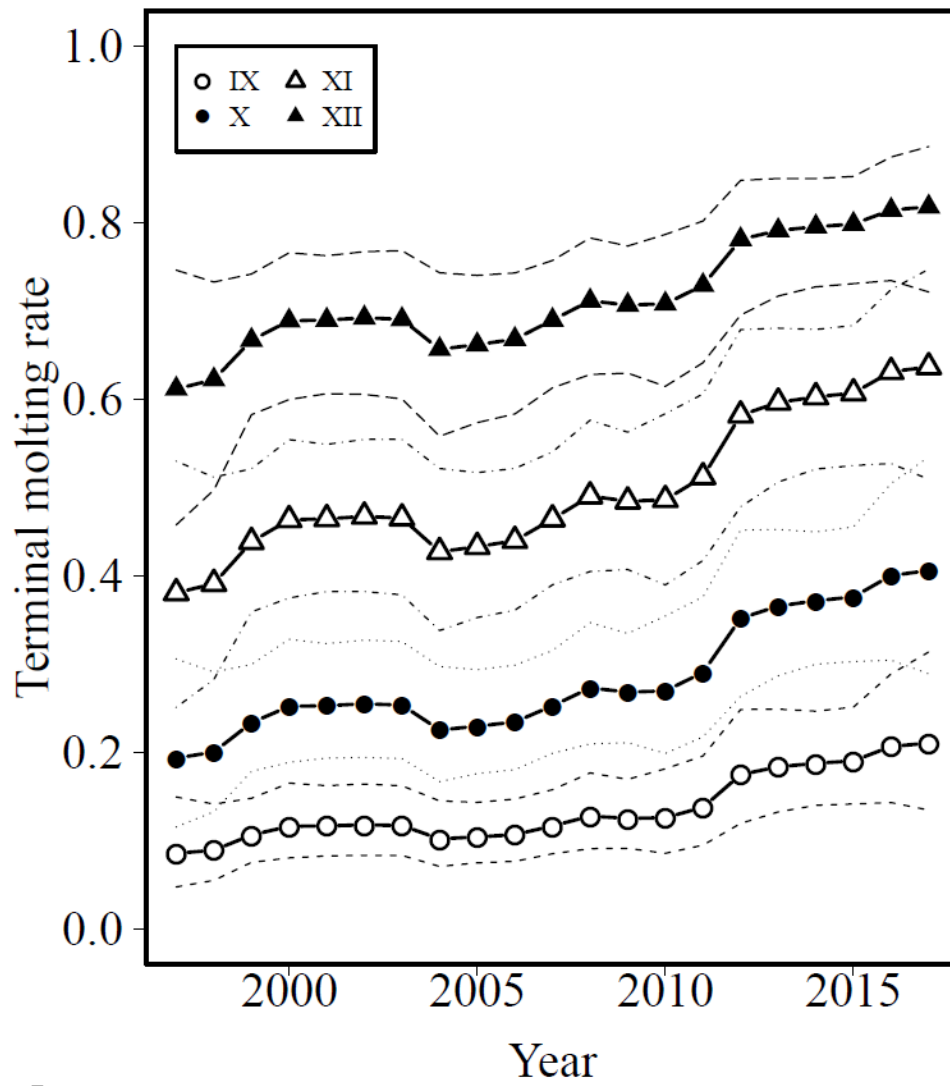
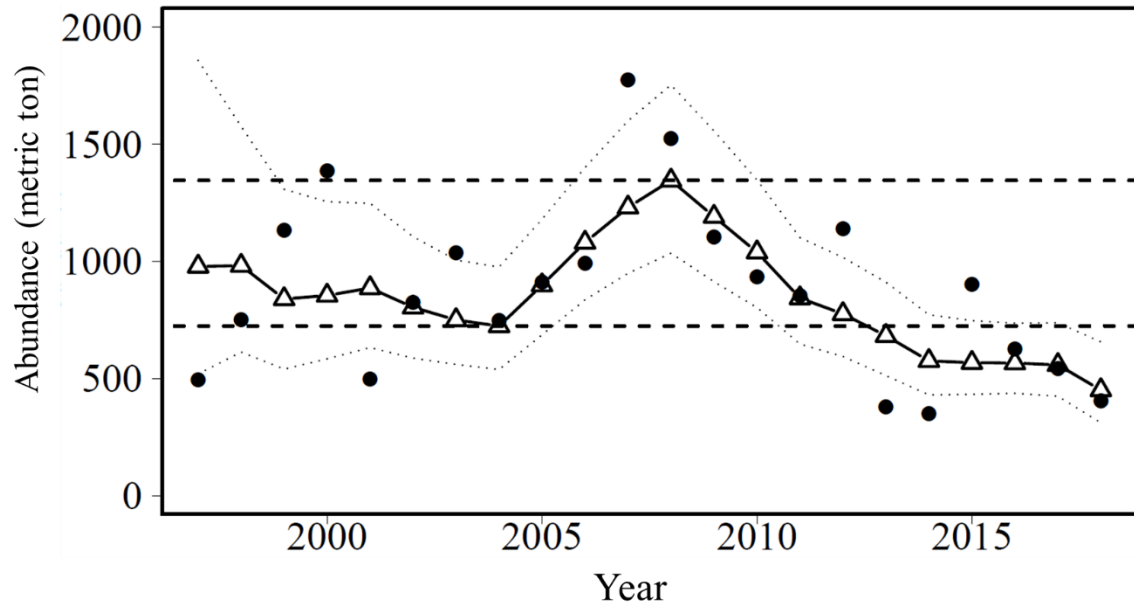


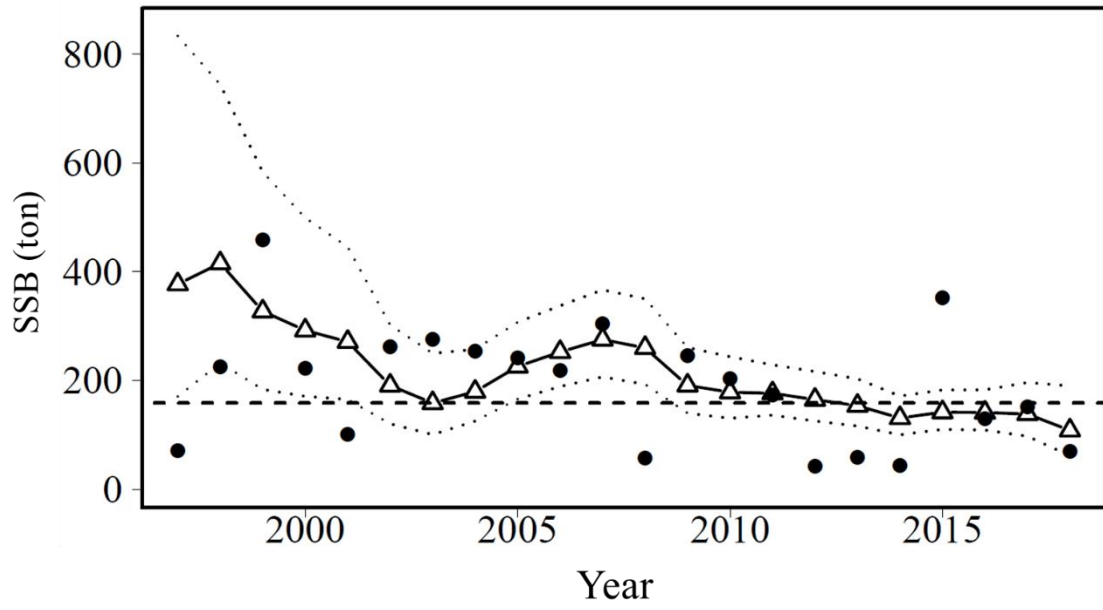
Fig. 5



902

903

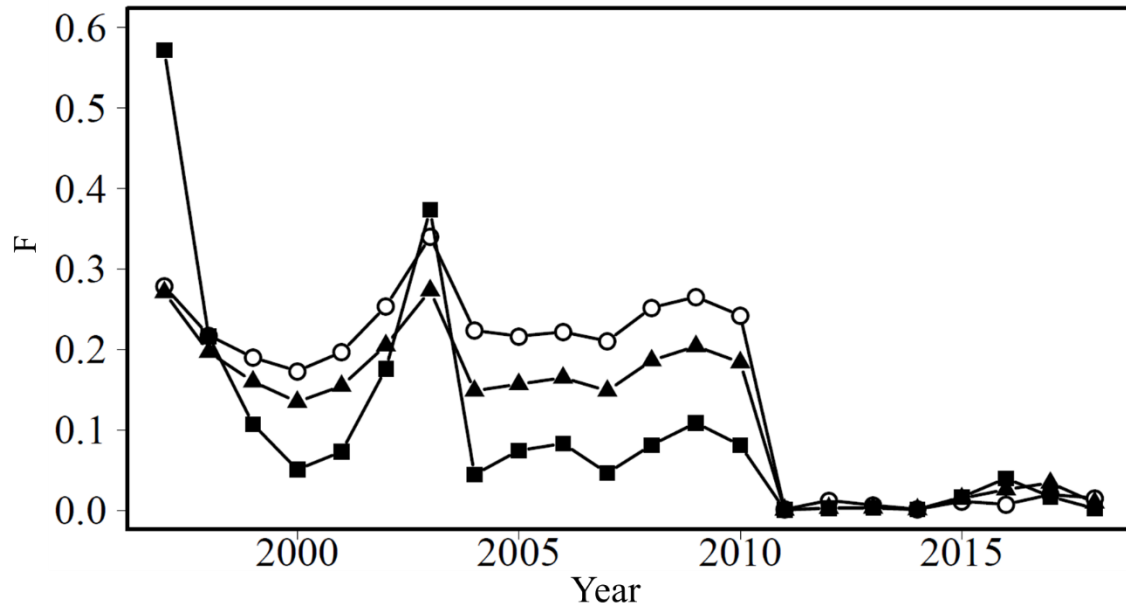
Fig. 6



904

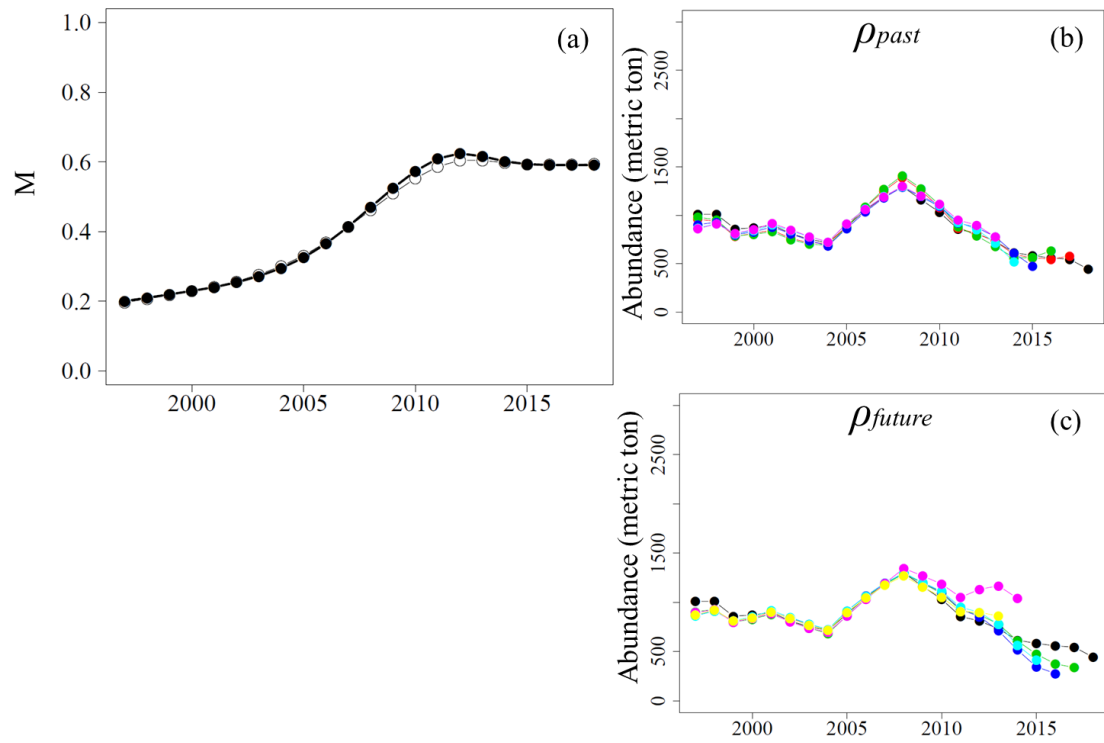
905

Fig. 7



906

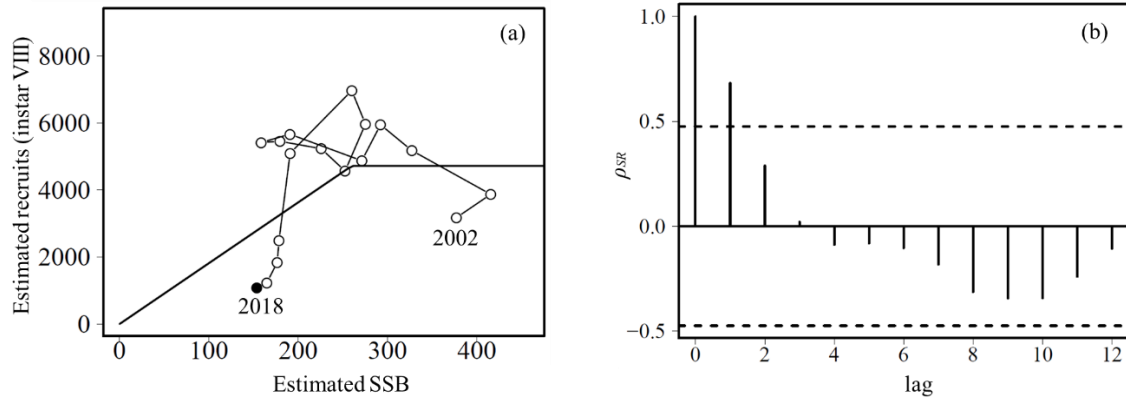
907 Fig. 8



908

909

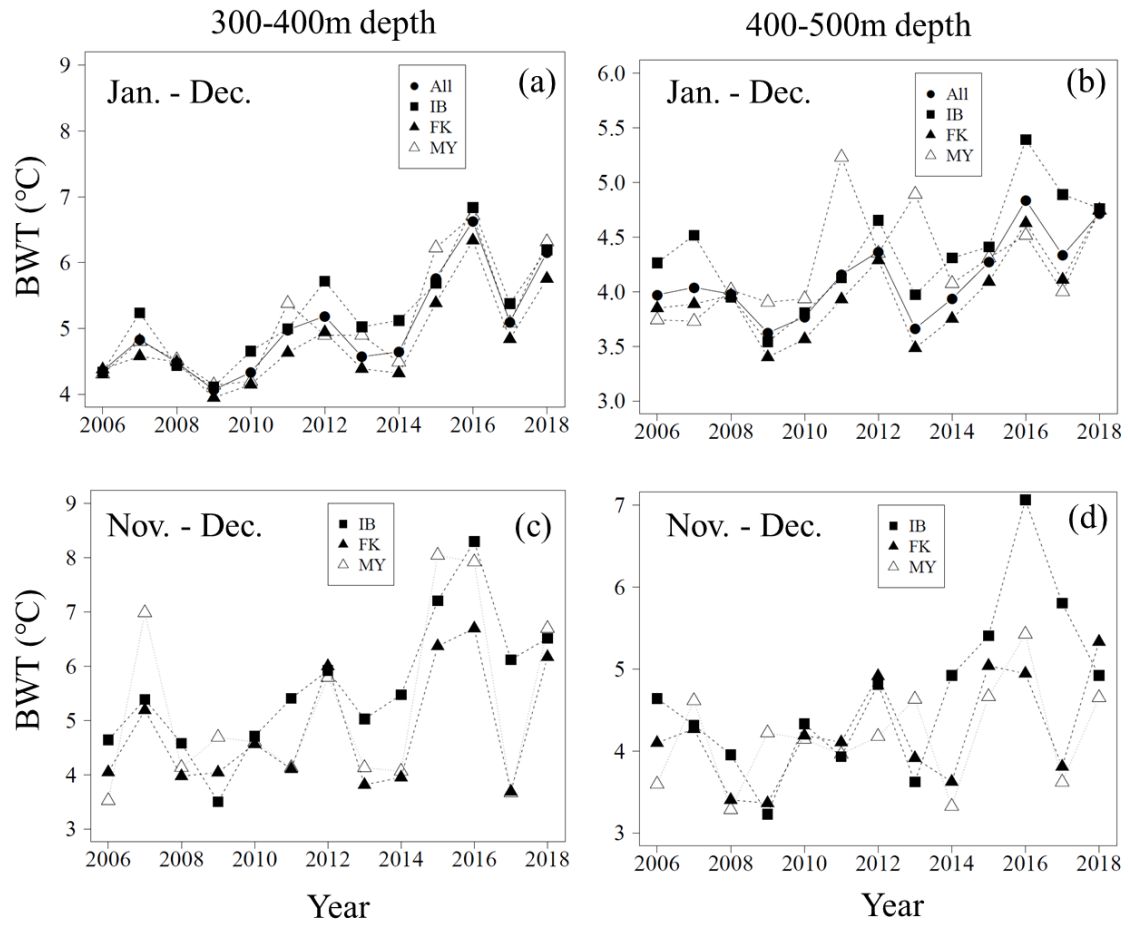
Fig. 9



910

911

Fig. 10



912

913

Fig. 11

914 Table 1

Sex	Instar categories in population model	CW intervals	Terminally molted	Fishable
Male	VIII	24 - 42	No	No
	IX	42 - 56	No	No
	X with not TM	56 - 74	No	No
	X with TM	56 - 74	Yes	No
	XI with not TM and not fishable	74 - 80	No	No
	XI with TM and not fishable	74 - 80	Yes	No
	XI with not TM and fishable	80 - 86	No	Yes
	XI with TM and fishable	80 - 86	Yes	Yes
	XII with not TM	86 - 98	No	Yes
	XII with TM	86 - 98	Yes	Yes
	XIII with not TM	98 -	No	Yes
	XIII with TM	98 - 110	Yes	Yes
	XIV with TM	110-	Yes	Yes
	Female	VIII	24 - 42	No
IX		42 - 56	No	No
X with not TM		56 - 74	No	No
XI with TM and fishable		-	Yes	Yes

915

916

917

918

919

920

921 Table 2

Variables/Types of difference	Number of combinations	Equation number
Mg	32	Supporting Information 2
Types of $M_{g,t}$	3	(1) and (2)
T_{Mg}	2	(29) and (30)
φ	2	(3)
T_{ρ}	2	(8)
$T_{\rho k}$	5	(8)
β_0	2	(10) and (11)
θ	2	(32)
Total	15,360	

922

923

924

925

926

927

928

929 Table 3

<i>M</i>	<i>Criterion</i>	<i>VIII</i>	<i>IX</i>	<i>X</i>	<i>XI</i>	<i>XII</i>	<i>XIII</i>	T_φ	T_{Mg}	T_ρ	θ	β	AIC/BIC	ρ_{past}	ρ_{future}
Const.	AIC	0	0	1	1	1	2	-	-	-	In	<i>t</i>	1147.3	-5.6	-8.5
	BIC												1345.2		
First	AIC	0	0	1	1	2	2	-	In	-	In	<i>t</i>	1064.5	0.2	66.3
	BIC												1254.2		
Second	AIC	0	0	0	0	0	0	-	-	-	In	<i>t</i>	1118.2	-12.5	-43.3
	BIC	0	0	0	0	0	0	-	-	-	-	<i>t</i>	1311.4	1.2	3.1

930

931

932

933

934

935

936

937 Table 4

Parameters	Estimates	Std.error	Either male or female
$\ln((\sigma_{k=1}^F)^2)$	-0.170	0.239	male
$\ln((\sigma_{k=2}^F)^2)$	-1.349	0.367	male
$\ln((\sigma_{k=3}^F)^2)$	-1.491	0.725	female
$T_{\sigma_{k=1}}^F$	0.660	0.368	male
$T_{\sigma_{k=2}}^F$	1.829	0.474	male
$T_{\sigma_{k=3}}^F$	2.104	0.750	female
$EQ_{k=1}$	-5.020	0.948	male
$EQ_{k=2}$	-5.996	0.396	male
$EQ_{k=3}$	-5.540	0.403	female
$\ln(\sigma_{M,g}^2)$	-2.998	0.771	both
$\ln(\tau_{a=11,u=0}^2)$	-0.994	0.467	male
$\ln(\tau_{a=11,u=1}^2)$	-0.934	0.220	male
$\ln(\tau_{a=12,u=0}^2)$	-0.787	0.329	male
$\ln(\tau_{a=12,u=1}^2)$	-1.076	0.209	male
$\ln(\tau_{a=13,u=0}^2)$	-0.221	0.210	male
$\ln(\tau_{a=13,u=1}^2)$	-1.100	0.231	male
$\ln(\tau_{a=14,u=1}^2)$	-0.332	0.166	male
$\ln(\tau_{a=11,u=1}^2)$	-1.299	0.372	female
$\ln(N_{a=9,u=0,t=1997})$	6.969	0.243	male
$\ln(N_{a=10,u=0,t=1997})$	6.335	0.243	male
$\ln(N_{a=10,u=1,t=1997})$	4.916	0.561	male
$\ln(N_{a=11,u=0,t=1997,74-80})$	5.352	0.352	male
$\ln(N_{a=11,u=1,t=1997,74-80})$	4.450	0.466	male
$\ln(N_{a=11,u=0,t=1997,80-86})$	5.023	0.350	male
$\ln(N_{a=11,u=1,t=1997,80-86})$	5.410	0.278	male
$\ln(N_{a=12,u=0,t=1997})$	4.714	0.342	male
$\ln(N_{a=12,u=1,t=1997})$	5.318	0.274	male
$\ln(N_{a=13,u=0,t=1997})$	3.308	0.586	male
$\ln(N_{a=13,u=1,t=1997})$	5.525	0.245	male
$\ln(N_{a=14,u=1,t=1997})$	4.937	0.300	male
$\ln(N_{a=9,u=0,t=1997})$	6.794	0.461	female
$\ln(N_{a=10,u=0,t=1997})$	7.613	0.492	female
$\ln(N_{a=11,u=0,t=1997})$	8.295	0.345	female
$\ln(\beta_1)$	-0.060	0.060	both
$\ln(\sigma_{\beta_0})$	-1.596	0.677	both
$T_{\rho,k=1}$	3.029	0.678	both
$T_{\rho,k=3}$	-1.179	0.312	both
T_r	-0.149	0.104	both
$\ln(\sigma_{rec}^2)$	-1.085	0.203	both
μ_{ω}	-0.803	0.089	both
$\ln(\sigma_{\omega}^2)$	-1.138	0.299	both

938

939

940 Table 5

Scenario	MSY	SSBmsy	M
1	598	331	0.21
2	$<10^{-8}$	$<10^{-8}$	0.59
3	29	188	0.43

941

942

943

944

945

946

947 **Supporting Information 1**

948 *Correction of CVs using Taylor's power law*

949

950 In a swept area method, the mean and standard error are equal when there is a sample at only one

951 station and no samples are obtained at other stations. The situation is simply shown in R code as below:

952

953 `> x <- c(5, 0, 0, 0, 0, 0)`

954 `> mean(x)`

955 `[1] 0.8333333`

956 `> sd(x)/sqrt((length(x)))`

957 `[1] 0.8333333`

958

959 Although the coefficient of variation (CV) was calculated as one in this case, the value could be higher

960 than expected. We used the CVs corrected by Taylor's power law (Taylor 1961) as the below regression

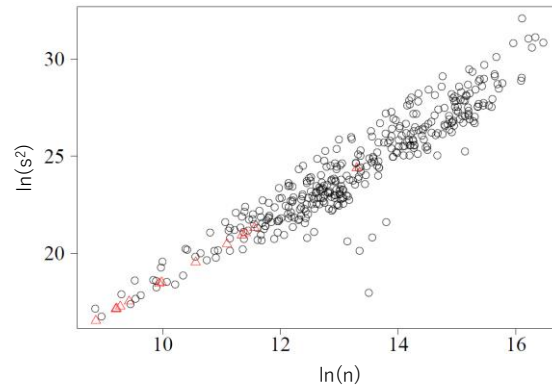
961 model:

962

963 $\ln(s_{a,u,t}^2) = \alpha_0 + \alpha_1 \times \ln(n_{a,u,t}),$ (A1)

964

965 where n is the observed number of snow crabs, s is their standard error, and the subscripts a , u , and t
966 show the same as in the article. The estimates were $\hat{\alpha}_0 = 0.828$ (SE = 0.464), $\hat{\alpha}_1 = 1.772$ (SE =



967 0.035), adjusted $R^2 = 0.88$ and the CVs were corrected using eq. A1 (Fig. A1). There was no change
968 in the best model before and after the correction.

969 Figure A1. The relationship between $\ln(n)$ and $\ln(s^2)$ (black circle). Red triangles show the corrected
970 standard errors using eq. A1.

971

972 **References**

973 Taylor LR (1961) Aggregation, variance and the mean. *Nature* 189:732–735

974

975 **Supporting Information 2**

976 *Combinations of age groups*

977 All the 32 combinations of age groups. If the numbers are the same in a combination, those instars

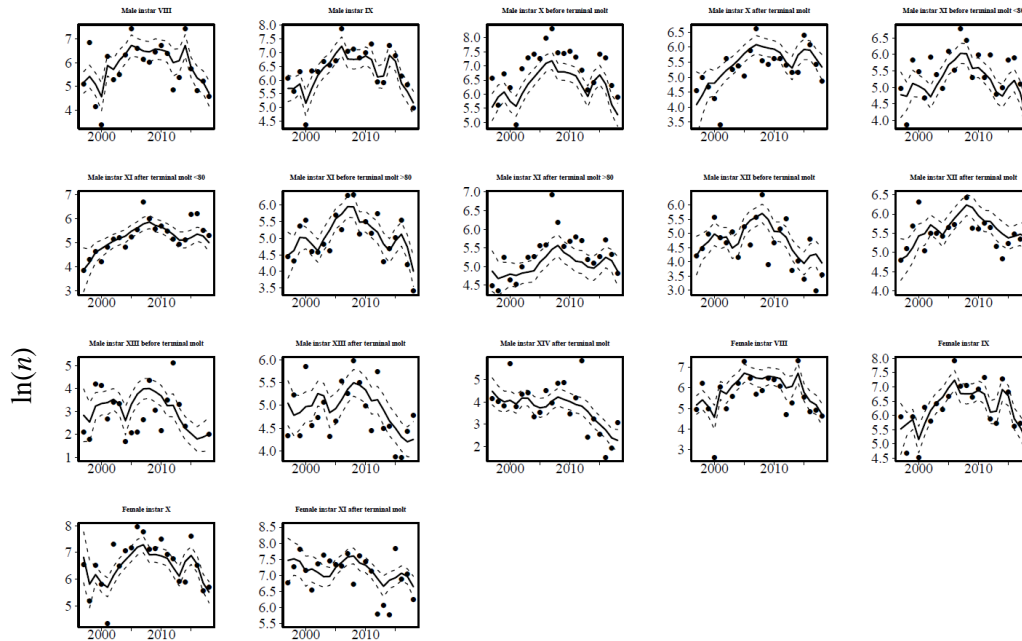
978 ($a=8, \dots, 13$) are included in the same age group. Mg equals Ma in the last combination (i.e., all the

979 instars take a different M).

<i>a/comb.</i> VIII	<i>g</i>					
	IX	X	XI	XII	XIII	
1	0	0	0	0	0	0
2	0	0	0	0	0	1
3	0	0	0	0	1	1
4	0	0	0	1	1	1
5	0	0	1	1	1	1
6	0	1	1	1	1	1
7	0	0	0	0	1	2
8	0	0	0	1	1	2
9	0	0	1	1	1	2
10	0	1	1	1	1	2
11	0	0	0	1	2	2
12	0	0	1	1	2	2
13	0	1	1	1	2	2
14	0	0	1	2	2	2
15	0	1	1	2	2	2
16	0	1	2	2	2	2
17	0	0	0	1	2	3
18	0	0	1	1	2	3
19	0	1	1	1	2	3
20	0	0	1	2	2	3
21	0	1	1	2	2	3
22	0	1	2	2	2	3
23	0	0	1	2	3	3
24	0	1	1	2	3	3
25	0	1	2	2	3	3
26	0	1	2	3	3	3
27	0	0	1	2	3	4
28	0	1	1	2	3	4
29	0	1	2	2	3	4
30	0	1	2	3	3	4
31	0	1	2	3	4	4
32	0	1	2	3	4	5

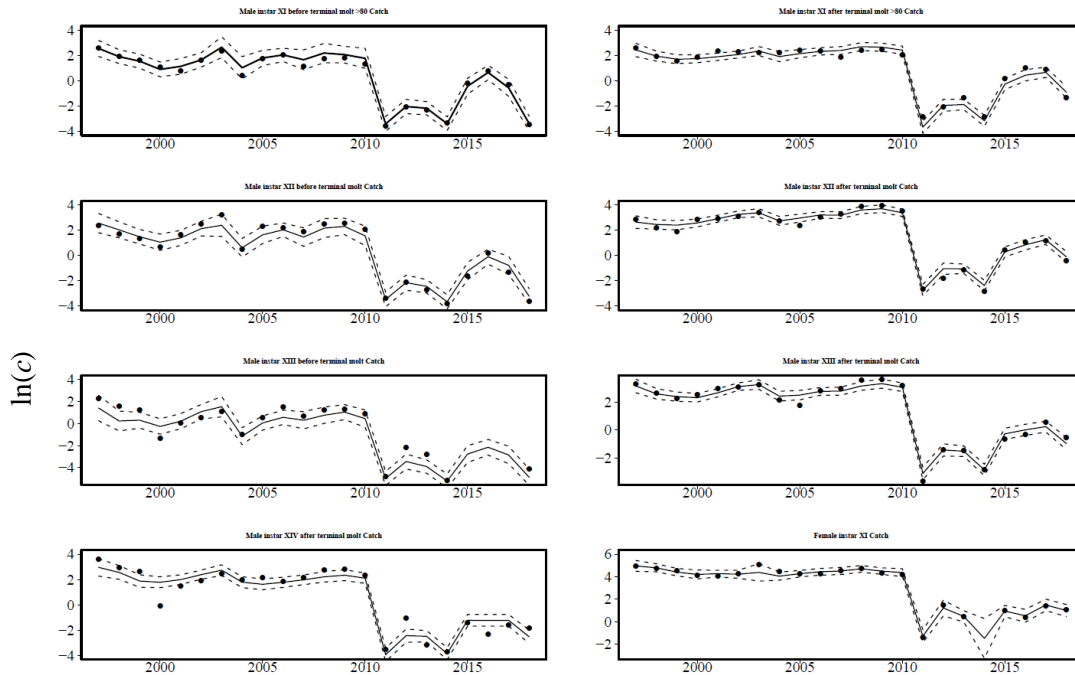
980 **Supporting Information 3**

981 *Result of fittings for observation*



982

983



984

985

986 **Supporting Information 4**

987 *Estimated bottom water temperatures*

988

989 Water temperatures at the maximum observed depth in the Tohoku region were extracted from the
990 conductivity, temperature, and depth (CTD) data obtained by prefectural fisheries experimental
991 stations and Fisheries Research and Education Agency in Japan. Then, we adopted bottom water
992 temperatures using the observed depth of water temperatures as follows: when the depth of the station
993 was ≤ 100 m, the temperatures of which the observed depth was within 10 m from the seabed were
994 adopted. Temperatures of which the observed depth was within 10% of the bottom depth of the seabed
995 were adopted when the depth of the station was > 100 m. The obtained bottom water temperatures
996 were interpolated to monthly gridded data of 5×5 min meshes weighed by time, distance, and depth
997 using a flexible Gaussian filter (Shimizu and Ito 1996).

998

999 **References**

1000 Shimizu Y, Ito S-I (1996) A new method to draw isotherms in the Tohoku offshore area: new
1001 interpolation method “flexible Gaussian filter.” Bull Tohoku Natl Fish Res Inst 58:105–117

1002

1003